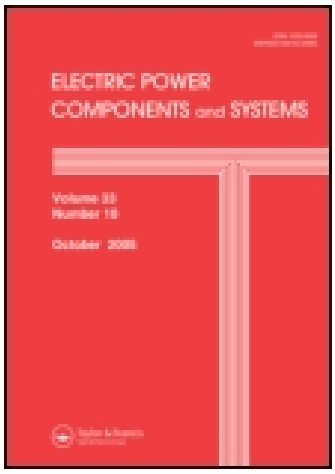

Electric Power Components and Systems
Publication details, including instructions for authors and subscription information:
http://www.tandfonline.com/loi/uemp20

Overview of Maximum Power Point Tracking Techniques for Photovoltaic Energy Production Systems

Eftichios Koutroulis[a] & Frede Blaabjerg[b]
[a] School of Electronic and Computer Engineering, Technical University of Crete, Chania, Greece
[b] Department of Energy Technology, Aalborg University, Aalborg, Denmark
Published online: 12 Jul 2015.

Electric Power Components and Systems, 43(12):1329–1351, 2015

ISSN: 1532-5008 print / 1532-5016 online
DOI: 10.1080/15325008.2015.1030517

Taylor & Francis
Taylor & Francis Group

Overview of Maximum Power Point Tracking Techniques for Photovoltaic Energy Production Systems

Eftichios Koutroulis[1] and Frede Blaabjerg[2]
[1]School of Electronic and Computer Engineering, Technical University of Crete, Chania, Greece
[2]Department of Energy Technology, Aalborg University, Aalborg, Denmark

CONTENTS

Abstract—A substantial growth of the installed photovoltaic systems capacity has occurred around the world during the last decade, thus enhancing the availability of electric energy in an environmentally friendly way. The maximum power point tracking technique enables maximization of the energy production of photovoltaic sources during stochastically varying solar irradiation and ambient temperature conditions. Thus, the overall efficiency of the photovoltaic energy production system is increased. Numerous techniques have been presented during the last decade for implementing the maximum power point tracking process in a photovoltaic system. This article provides an overview of the operating principles of these techniques, which are suited for either uniform or non-uniform solar irradiation conditions. The operational characteristics and implementation requirements of these maximum power point tracking methods are also analyzed to demonstrate their performance features.

1. INTRODUCTION

Motivated by the concerns on environmental protection (sustainability) and energy availability, the installation of photovoltaic (PV) energy-productions systems has been increased substantially during the last years. The falling prices of PV modules and more highly efficient power conversion have assisted that direction by enhancing the economic viability of the installed PV systems. More than 38 GW of new PV capacity was installed across the world during 2013, thus reaching a worldwide cumulative installed capacity of 138.9 GW during that year [1].

A basic block diagram of a PV energy production system is shown in Figure 1, with a PV array comprising a number of PV modules, a power converter, and also a control unit. The PV source is connected to a DC/DC or DC/AC power converter, respectively, interfacing the PV generated power to the load, which is typically connected to the electrical grid, or operating in a stand-alone-mode (*e.g.*, using a battery bank) [2, 3]. The pulse-width modulation (PWM) controller of the control unit

Keywords: photovoltaic, maximum power point tracking, control, solar energy management, optimization, PV module, PV array, MPPT
Received 24 November 2014; accepted 10 March 2015
Address correspondence to Dr. Eftichios Koutroulis, School of Electronic and Computer Engineering, Technical University of Crete, Chania, GR -73100, Greece. E-mail: efkout@electronics.tuc.gr
Color versions of one or more of the figures in the article can be found online at www.tandfonline.com/uemp.

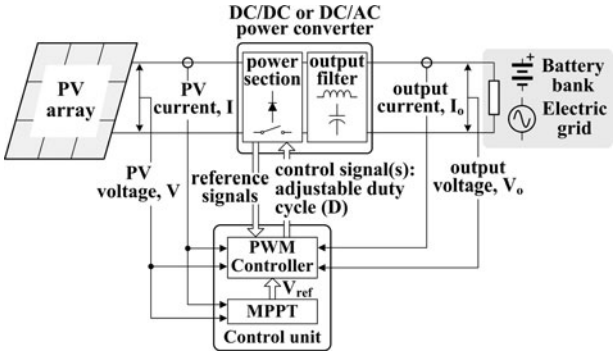

FIGURE 1. Block diagram of a PV energy production system.

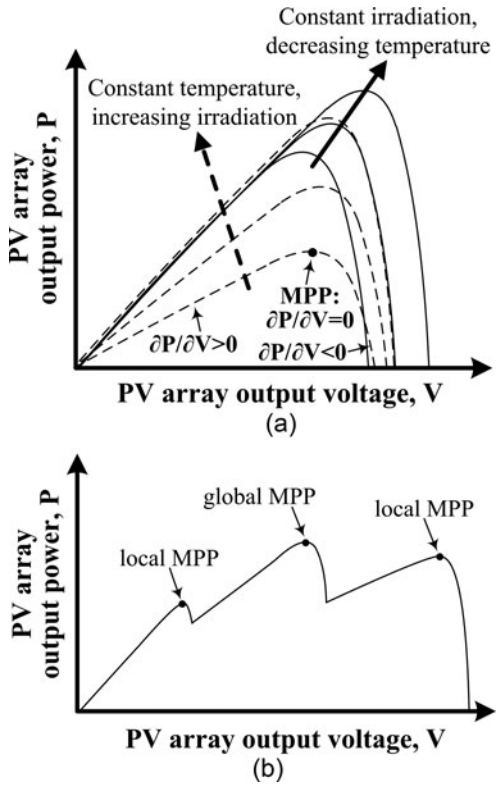

FIGURE 2. Examples of the power-voltage characteristics of a PV array: (a) under uniform solar irradiation conditions and (b) under partial shading conditions.

is responsible for producing the appropriate control signals (with an adjustable duty cycle) that drive the power switches (*e.g.*, metal-oxide-semiconductor field-effect transistor (MOSFETs), insulated-gate bipolar transistors [IGBTs], etc.) of the power converter. Its operation is based on measurements of the input/output voltage and current, as well as of internal reference signals of the power converter.

Examples of the power-voltage characteristics of a PV array under various atmospheric conditions are illustrated in Figure 2(a) for the case that the same amount of solar irradiation is incident on all PV modules of the PV array [2]. It is observed that the power-voltage curves exhibit a unique point where the power produced by the PV module is maximized (*i.e.*, the maximum power point [MPP]). However, in the case that the solar irradiation, which is incident on one or more of the PV modules, is different (*e.g.*, due to dust, shading caused by buildings or trees, etc.), then the power-voltage characteristic of the PV array is distorted, exhibiting one or more local MPPs (Figure 2(b)) [4]. Among them, the operating point where the output power is maximized corresponds to the global MPP of the PV array. However, the power generated by the PV array at the global MPP is less than the sum of the power values produced by the individual PV modules when operating at their respective MPPs. The number and position of the local MPPs on the power-voltage curve of the PV array depend on both the configuration (*i.e.*, connection in series and/or parallel) of the PV modules in the PV array and the time-varying form of the shading pattern on the surface of the PV modules.

As shown in Figure 3, the solar irradiance and ambient temperature conditions exhibit a stochastic variation during a year, a day, and an hour, respectively. During these operating conditions, the location of the MPP(s) on the power-voltage curve of the PV array varies accordingly. Thus, an appropriate operation is incorporated in the control unit of the PV energy production system, as also shown in Figure 1, for continuously adjusting the operation of the power converter under the stochastically changing weather conditions, such that the operating point of the PV array, which is determined by its output voltage and current, always corresponds to the global MPP. This process is called MPP tracking (MPPT). Employing an MPPT process is indispensable in every PV energy production system to ensure that the available PV energy production potential is optimally exploited, thus maximizing the energy production, and by that reducing the cost of the energy generated. Depending on the type of PV application, the MPPT process operates by controlling the power converter of the PV system based on measurements of the PV array output voltage and current, and it is appropriately integrated into the energy management algorithm, which is executed by the control unit. For example, in PV systems containing a battery energy-storage unit, the battery charging control is also performed for protection from overcharging [2]. Also, in the case of grid-connected PV inverters, the MPPT process may be executed only as long as the PV-generated power is less than a predefined upper limit [5]. Otherwise, the MPPT algorithm is deactivated and the power produced by the PV source is regulated to remain at that limit. By controlling the feed-in power of the electric grid, this control method enables better utilization of the electric grid

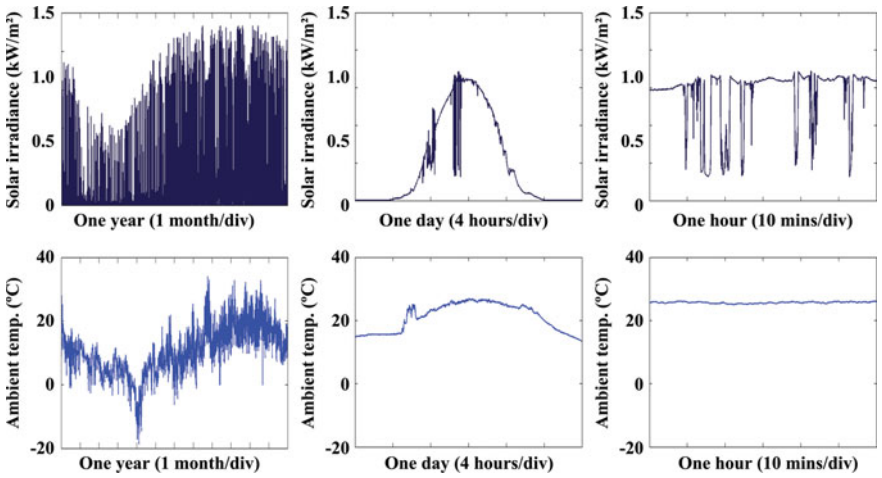

FIGURE 3. Examples of the variation of solar irradiance and ambient temperature during a year, a day, and an hour, respectively.

and increases the utilization factor of the PV inverter; simultaneously, the thermal loading of its power semiconductors is reduced, and their reliability is also increased.

Various methods have been presented in the research literature for performing the MPPT process under either uniform incident solar irradiation or partial shading conditions. Each of these methods is based on a different operating principle and exhibits different hardware implementation requirements and performance [6–12]. In this article, the operation and modeling of PV modules and arrays are initially described. Then, the operating principles of the existing MPPT methods, which are suited for either uniform or non-uniform solar irradiation conditions, are analyzed with a primary focus on the MPPT techniques developed during the last years. An overview of these MPPT methods is presented in Figure 4. Their implementation requirements and operational characteristics are also analyzed to demonstrate their performance features, thus assisting the designers of PV power processing systems to select the MPPT technique that is most suitable for incorporation in their target PV application.

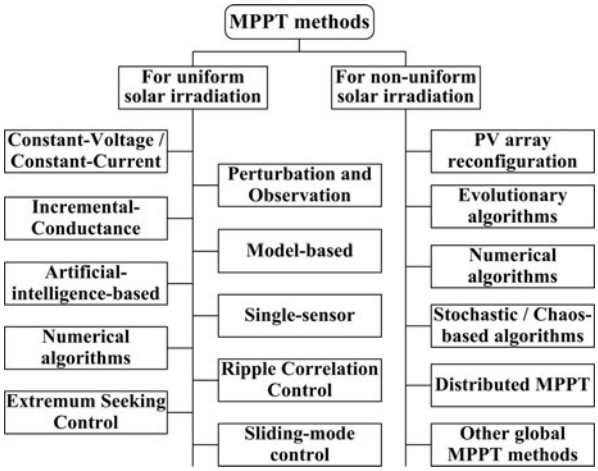

FIGURE 4. Overview of MPPT methods for PV arrays operating under uniform or non-uniform solar irradiation conditions.

2. THE OPERATION AND MODELING OF PV MODULES AND ARRAYS

The elementary structural units of a PV source are the solar cells, which operate according to the PV effect [13]. The photons of the incident solar irradiation are absorbed by the semiconducting material of the solar cell, exciting the generation of electron-hole pairs, which results in the flow of electric current when the solar cell is connected to an electric circuit. Multiple solar cells are connected electrically in series and parallel, thus forming a PV module. A PV array consists of multiple PV modules, also connected in series and parallel, to comply with the voltage and power level requirements of the PV system. Currently, the PV modules that are available on the market are constructed using such materials as multicrystalline silicon and mono-crystalline silicon, as well as by employing thin-film technologies based on cadmium telluride (CdTe), copper indium gallium selenide (CIGS), and amorphous silicon [14]. The multi-junction solar cells are expensive, but they have the ability to operate under a high level of solar irradiation intensity with high efficiency; thus, they are mostly used in space and high-concentrating PV applications. Also, new solar cell technologies, such as dye-sensitized and organic cells, are under development [15].

	Multi-crystalline silicon	Mono-crystalline silicon	CdTe	CIGS	Amorphous silicon
Average efficiency (%)	14.1–15.4	14.8–17.0	11.9–12.7	11.7–12.0	7.0–10.2
Degradation rate of power production (%/year)	0.61–0.64	0.36–0.47	0.40–3.33	0.96–1.44	0.87–0.96

TABLE 1. Comparison of commercially available PV module technologies

A comparison of the primary commercially available PV module technologies in terms of efficiency and degradation rate of power production is presented in Table 1 [16, 17].

Various models have been presented in the scientific literature for describing the current-voltage characteristic of a PV source to estimate its performance under real operating conditions [18]. Due to its simplicity and ability to provide sufficient accuracy for a wide variety of studies and applications, the single-diode five-parameter model is widely adopted (Figure 5(a)). According to this model, output current I and power P of a PV source are given by the following equations [19]:

$$I = I_{ph} - I_s \cdot \left(e^{\frac{q \cdot (V + I \cdot R_s)}{N_s \cdot n \cdot k \cdot T}} - 1 \right) - \frac{V + I \cdot R_s}{R_p}, \quad (1)$$

$$P = V \cdot I, \quad (2)$$

where

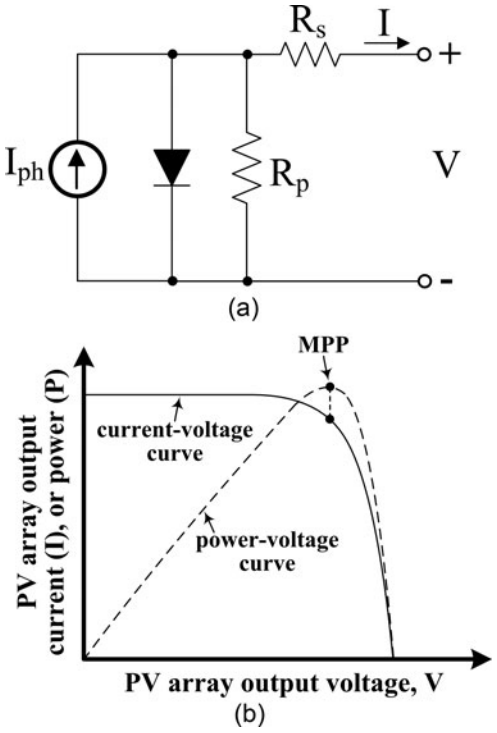

FIGURE 5. Single-diode model of a PV module/array: (a) equivalent circuit and (b) corresponding current-voltage and power-voltage characteristics.

V is the output voltage of the PV source,
I_{ph} is the photocurrent,
I_s is the reverse saturation current,
q is the electron charge ($q = 1.602176565 \cdot 10^{-19}$ C),
n is the ideality factor of the solar cells,
k is the Boltzmann constant ($k = 1.3806488 \cdot 10^{-23}$ J/K),
N_s is the number of solar cells connected in series,
T (°C) is the temperature of the solar cells, and
R_s and R_p are the series and parallel resistances of the PV source, respectively.

The values of I_{ph} and T in Eq. (1) depend on the solar irradiation and ambient temperature mission profile [13] (*e.g.*, see Figure 3). The impact of R_p is usually neglected, while due to the small value of R_s, the short-circuit current of the PV module/array, $I_{sc} = I|_{V=0}$, is approximately equal to I_{ph}. The short-circuit current I_{sc} depends on the solar irradiance, which is incident on the surface of the PV source. The open-circuit voltage of the PV source V_{oc} is derived by setting $I = 0$ in Eq. (1), and its value is affected significantly by the temperature of the solar cells. The current-voltage and power-voltage characteristics of a PV module/array are shown in Figure 5(b). The location of the MPP on these curves is also illustrated in Figure 5(b). When the meteorological conditions vary, the shape of the current-voltage and power-voltage characteristics is also modified according to Eqs. (1) and (2), respectively, and the position of the MPP changes (see Figure 2(a)).

The PV modules/array model described above can either be used in simulation studies for evaluating the performance of a PV system under uniform or non-uniform solar irradiance at the individual PV modules of the PV source, given the meteorological conditions at the installation site (*e.g.*, Figure 2), or for implementing an MPPT method, as described next.

3. MPPT METHODS FOR PV ARRAYS OPERATING UNDER UNIFORM SOLAR IRRADIATION CONDITIONS

This class of MPPT techniques is suited for application in cases that the PV modules of the PV source operate under uniform solar irradiation conditions. In such a case, the power-voltage characteristic of the PV source exhibits a unique MPP.

However, due to the short- and long-term variability of solar irradiation and ambient temperature (see Figure 3), the position of the MPP will be changed accordingly. Thus, the application of an MPPT control algorithm is required, which is capable to guarantee fast convergence to the continuously moving MPP of the PV source to maximize the energy production of the PV system. The operating principles of alternative techniques that belong to this class of MPPT methods (see Figure 4) along with a comparison of their operational characteristics are presented next.

3.1. Constant-voltage and Constant-current MPPT

The constant-voltage (also referred as fractional open-circuit voltage) MPPT technique is based on the assumption that the ratio of the MPP voltage to the open-circuit voltage of a PV module remains relatively constant at 70–85% [20, 21]. Thus, by periodically disconnecting the power converter (Figure 1) from the PV array, the output current of the PV array is set to zero, and the resulting open-circuit voltage is measured. In the constant-current (or fractional short-circuit current) MPPT method, a similar approach is adopted [22]. In this case, the MPPT process is based on the assumption that the MPP power is proportional to the short-circuit current, which is measured by periodically setting the PV module/array under short-circuit conditions through a power switch. In both the constant-voltage and constant-current MPPT methods, the corresponding MPP voltage is calculated by the control unit according to the measurements of the open-circuit voltage and short-circuit current, respectively, and then the power converter is regulated to operate at that point.

The constant-voltage and constant-current MPPT methods require only one sensor for their implementation (*i.e.*, a voltage or current sensor, respectively), but the periodic interruption of the PV source operation for measuring the open-circuit voltage/short-circuit current results in power loss. In both of these methods, the MPPT accuracy is affected by the accuracy of knowing the value of the proportionality factors between the open-circuit voltage and short-circuit current, respectively, with the corresponding values at the MPP for the specific PV module/array used in each installation, as well as their variations with temperature and aging.

3.2. Perturbation and Observation (P&O) MPPT

The P&O MPPT method is based on the property that the derivative of the power-voltage characteristic of the PV module/array is positive at the left side and negative at the right side (see Figure 2(a)), while at the MPP, it holds that

$$\frac{\partial P}{\partial V} = 0, \tag{3}$$

where P and V are the output power and voltage, respectively, of the PV module/array.

During execution of the P&O MPPT process, the output voltage and current of the PV module/array are periodically sampled at consecutive sampling steps to calculate the corresponding output power, as well as the power derivative with voltage. The MPPT process is performed by adjusting the reference signal of the power converter PWM controller (see Figure 1), V_{ref}, based on the sign of $\frac{\partial P}{\partial V}$, according to the following equation:

$$V_{ref}(k) = V_{ref}(k-1) + \alpha \cdot sign\left(\frac{\partial P}{\partial V}(k)\right), \tag{4}$$

where k and $k-1$ are consecutive time steps, $\alpha > 0$ is a constant determining the speed of convergence to the MPP, and the function $sign(\cdot)$ is defined as follows:

$$sign(x) = \begin{cases} 1 & \text{if } x > 0 \\ -1 & \text{if } x < 0 \end{cases}. \tag{5}$$

The PV module/array output voltage is regulated to the desired value, which is determined by V_{ref} according to Eq. (4), using either a proportional-integral (PI) or, *e.g.*, a fuzzy logic controller. The latter has the advantage of providing a better response under dynamic conditions [23]. Under steady-state conditions, the operating point of the PV module/array oscillates around the MPP with an amplitude determined by the value of α in Eq. (4). Increasing the perturbation step enables faster convergence to the MPP under changing solar irradiation and/or ambient temperature conditions, but it increases the steady-state oscillations around the MPP, and thus it may result in power loss.

An MPPT system based on the P&O method can be developed by implementing Eq. (4) either in the form of an algorithm executed by a microcontroller or digital signal processing (DSP) unit or using mixed-signal circuits. A flowchart of the P&O MPPT algorithm based on the procedure proposed in [24], which can be executed by a microcontroller or DSP device of the control unit, is presented in Figure 6. The process shown in Figure 6 is executed iteratively until the value of gradient $\frac{\partial P}{\partial V}$ drops below a predefined threshold, indicating that convergence close to the MPP has been achieved with the desired accuracy.

A methodology for the design of the control unit, such that the P&O MPPT process operates with the optimal values of step-size and perturbation period, was proposed in [25]. The optimal perturbation period was calculated in [26] for adapting to the time-varying meteorological conditions using a field-programmable gate array (FPGA) control unit, which executes the P&O-based MPPT process. An algorithm for dynamically adapting the perturbation size, according to the solar

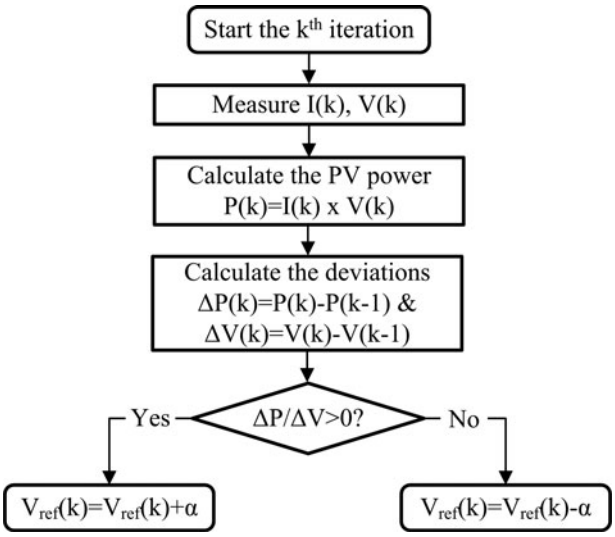

FIGURE 6. A flow-chart of the algorithm implementing the P&O MPPT process based on the procedure proposed in C. Hua et al., IEEE Trans. IE-45(1), p. 99, 1998.

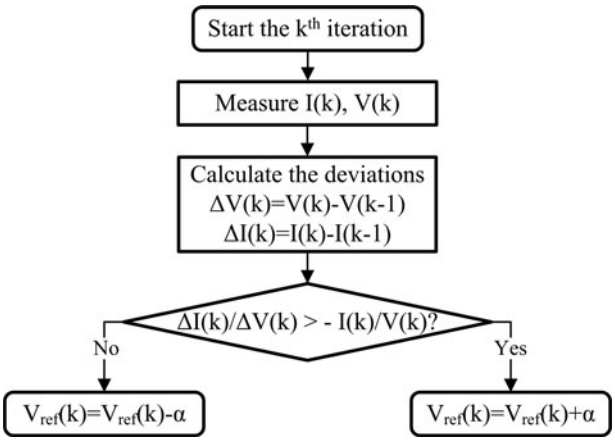

FIGURE 7. A flowchart of the InC MPPT algorithm based on the procedure presented in M.A. Elgendy et al., IEEE Trans. SE-4(1), p. 108, 2013.

irradiation conditions was presented in [27] for increasing the response speed of the P&O algorithm and reducing the steady-state oscillation around the MPP. The short-circuit current of the PV source was estimated in [28] during the execution of the P&O algorithm by applying the measured values of the current and voltage in the single-diode model of the PV modules. The resulting value is used to detect whether a variation of the PV source output power is due to a change of the solar irradiation conditions or the MPPT process itself.

The P&O method is characterized by its operational and implementation simplicity. However, it exhibits a slow convergence speed under varying solar irradiation conditions, and its performance may also be affected by system noise.

3.3. Incremental Conductance (InC) MPPT

At the MPP of the PV source, it holds that

$$\frac{\partial P}{\partial V} = 0 \quad \Rightarrow \quad \frac{\partial (I \cdot V)}{\partial V} = I + \frac{\partial I}{\partial V} V = 0 \quad \Rightarrow \quad \frac{\partial I}{\partial V} = -\frac{I}{V}, \tag{6}$$

where I is the output current of the PV array.

Due to the shape of the current-voltage characteristic of the PV module/array in Figure 5(b), the value of $\frac{\partial I}{\partial V}$ is higher than $-\frac{I}{V}$ at the left side of the MPP and lower than $-\frac{I}{V}$ at its right side. The InC MPPT technique operates by measuring the PV module/array output voltage and current and comparing the value of $\frac{\partial I}{\partial V}$ with $-\frac{I}{V}$. Then the power converter is controlled based on the result of this comparison, according to the flowchart illustrated in Figure 7, which is based on the procedure presented in [29]. Similarly to the P&O process, the execution of the algorithm shown in Figure 7 is iteratively repeated until the difference between $\frac{\partial I}{\partial V}$ and $-\frac{I}{V}$ is less than a predefined value, which indicates that the MPP has been tracked with an acceptable accuracy.

Alternatively, the InC method may be implemented by controlling the power converter according to the sign of $I + \frac{\partial I}{\partial V} V$ such that its value is adjusted to zero as dictated by (6).

Although the InC and P&O MPPT methods are based on the same operating principle, the former is implemented by using the individual measurements of the PV array output voltage and current, thus not requiring the computation of the corresponding output power. A variation of the InC algorithm, employing a dynamic adaptation of the step size during the tracking process, was proposed in [30].

In [31], it was demonstrated through experimental testing that the P&O and InC MPPT methods exhibit similar performances under both static and dynamic conditions.

3.4. Model-based MPPT

The operation of model-based MPPT methods is based on measuring the PV module/array output voltage and current at multiple operating points [32]. Using the resulting measurements, parameters I_{ph}, I_s, V_T, and R_s, respectively, of the single-diode model of the PV source, which has been described in Section 2, are initially estimated (the shunt resistance R_p is neglected). Then Eq. (1) is used to calculate the voltage and current of the PV source at the operating point, where the derivative of power with respect to the voltage is equal to zero (*i.e.*, MPP) by applying numerical techniques (*e.g.*, Newton–Raphson method). A similar approach has also been employed in [33], where successive measurements of the PV

module output voltage are iteratively applied in a simplified empirical mathematical model of the PV module, until a convergence to the MPP has been achieved.

In [34], analytical equations are derived that enable calculation of the PV module current and voltage at the MPP, as follows:

$$I_m = I_{1m} - \frac{V_{1m}}{R_p}, \tag{7}$$

$$V_m = V_{1m} - I_m R_s, \tag{8}$$

where

$$V_{1m} = n\alpha V_T \left[W\left(\frac{I_{ph} \cdot exp(1)}{I_s} \right) - 1 \right], \tag{9}$$

and $I_m = I|_{MPP}$ is the PV module current at the MPP, $V_m = V|_{MPP}$ is the PV module voltage at the MPP, n is the number of PV cells connected in series within the PV module, α is the quality factor, and $W(\cdot)$ is the Lambert function.

To apply this method, the value of I_{ph} is estimated from Eq. (1) using measurements of the PV module output current and voltage at an operating point away from the open-circuit voltage. When using this technique, the accuracy of predicting the MPP voltage and current is highly affected by the accuracy of estimating the PV module temperature, which affects the values of V_T and I_s applied in Eqs. (1) and (9). Also, due to the complexity of the computations required for calculating the MPP voltage or current, a microcontroller or DSP unit is required for the implementation of such an MPPT scheme, while additionally, the response speed of the MPP control algorithm is relatively low. However, due to the elimination of oscillations around the MPP, the MPPT units of this type achieve a better steady-state response and are mostly attractive in cases of continuously changing the solar irradiation conditions (*e.g.*, solar-powered electric vehicles). Instead of solving a set of equations in real time, a lookup table, which has been formed off-line, may also be used for calculating the MPP voltage [35], but this method is also characterized by computational complexity and requires knowledge of the operational characteristics of the PV source. In [36], the output of an MPPT subsystem operating according to the InC method is added to the output of a model-based MPP tracker, thus forming a hybrid MPPT controller.

The model-based MPPT techniques have the advantage of not disconnecting the PV source during the execution of the MPPT process. The accuracy of the model-based MPPT method is affected by the accuracy of the single-diode model of the PV source, as well as by the aging of the PV modules, which results in the modification of the values of the PV module operating parameters during the PV system operational lifetime period.

3.5. Artificial Intelligence-based MPPT

Artificial intelligence techniques, such as neural networks and fuzzy logic, have also been applied for performing the MPPT process. In the former case, measurements of solar irradiation and ambient temperature are input into an artificial neural network (ANN), and the corresponding optimal value of the DC/DC power converter duty cycle is estimated, as shown in Figure 8(a), which is based on the structure presented in [37]. To derive accurate results, the ANN must have been trained using a large amount of measurements prior to its real-time operation in the MPPT control unit [38], which is a disadvantage.

The controllers based on fuzzy logic have the ability to calculate the value of the power converter control signal (*e.g.*, duty cycle) for achieving operation at the MPP using measurements of an error signal e (*e.g.*, $e = \frac{\partial P}{\partial I}$, $e = \frac{\partial P}{\partial V}$ or $e = \frac{\partial I}{\partial V} + \frac{I}{V}$), as well as its variation with time (*i.e.*, Δe) [39, 40]. The structure of an MPPT scheme, employing a fuzzy logic controller based on the method proposed in [40], is presented in Figure 8(b). The values of e and Δe are assigned by the fuzzy logic-based controller to linguistic variables, such as "negative big" (NB), "positive small" (PS), etc., and the appropriate membership functions are applied. Based on the values resulting by this transformation, a lookup table that contains the desired control rules is used to calculate the output of the controller in the form of alternative linguistic variables, which are then combined through the corresponding membership functions into

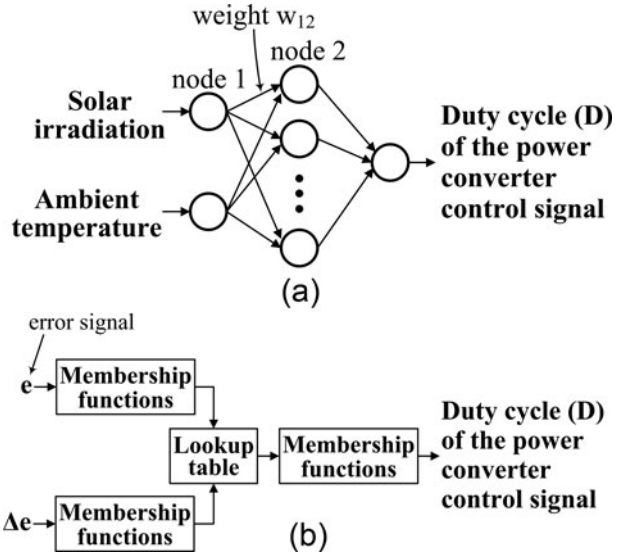

FIGURE 8. The structure of artificial-intelligence-based techniques for MPPT: (a) Artificial Neural Network based on the architecture presented in S. Charfi et al., 5th IREC, p. 1, 2014 and (b) Fuzzy logic controller based on the method proposed in M. Adly et al., 7th ICIEA, p. 113, 2012.

a numerical value (defuzzification stage), thus producing the duty cycle of the control signal driving the power converter such that the MPP is tracked. The fuzzy logic controllers have the advantage of not requiring knowledge of the exact model of the system under control. However, to obtain effective performance, expert knowledge is required for forming the membership functions and rule sets. Thus, optimization algorithms, such as genetic algorithms (GAs), ant colony optimization, etc., have been applied for tuning the operational parameters of fuzzy logic controllers [40], while in [38], the structure of an ANN is exploited for that purpose.

3.6. Single-sensor MPPT

The implementation of P&O and InC methods requires measurement of the PV module/array output current. The accuracy of current measurements is affected by the current sensor bandwidth and switching ripple imposed on the PV source output current due to the switching operation of the power converter. Additionally, the use of a current sensor increases the cost and power consumption of the MPPT control unit.

As analyzed in [41], the output power of the PV module/array is given by

$$P = V \cdot I = V \cdot \frac{V}{R_{in}} = k \cdot V^2, \tag{10}$$

where R_{in} is the input resistance of the power converter, which is a function of the duty cycle of the control signal driving the power converter, and $k = \frac{1}{R_{in}}$.

The value of V in Eq. (10) also depends on R_{in}. Thus, by modifying the control signal duty cycle, this will affect the resulting operating values of both V and P. The power produced by the PV source can be calculated by applying the measurements of the PV module/array output voltage in Eq. (10), thus avoiding the direct measurement of the corresponding output current. Using the calculated value of P, the P&O algorithm may be applied for executing the MPPT process.

In [42], a flyback inverter, operating in the discontinuous conduction mode, is connected at the output of the PV module for interfacing the PV-generated power to the electric grid. The output power of the PV module (*i.e.*, $P = V \cdot I$) is calculated by measuring the PV module output voltage and also calculating the PV source output current using the following equation (assuming a loss-less power converter):

$$I = \frac{1}{4} \cdot \frac{D_{\max}^2 \cdot T_s}{L_m} \cdot V, \tag{11}$$

where $D_{\max}$ is the maximum value of the primary-switch duty cycle during the half-period of the electric grid voltage, T_s is the switching period, and L_m is the magnetizing inductance of the isolation transformer incorporated into the flyback inverter circuit.

A P&O algorithm is also applied in this case for executing the MPPT process using the calculated values of I (by Eq. (11)) and P.

The accuracy of the single-sensor MPPT approaches is affected by the deviation of the operation of the practical power converter circuit from that predicted by the theoretical equations (Eqs. (10) and (11), respectively) due to the tolerance of the electric/electronic components values, circuit parasitics, etc. The MPPT accuracy of this method can be improved if the MPPT control unit is modified such that the aforementioned deviation is compensated by employing a suitable model of the power converter, but the complexity of the control unit would also be increased in that case.

3.7. MPPT Methods Based on Numerical Optimization Algorithms

A simple approach for deriving the position of a PV source MPP is to apply an exhaustive-search process, where the entire power-voltage characteristic is sequentially scanned. By measuring and comparing the power production levels at the individual operating points that the PV source is set to operate at during power-voltage curve scanning, the MPP position can be detected. Since this process requires a large number of search steps to be executed, which results in power loss until the tracking process has been accomplished, various MPPT algorithms based on numerical optimization techniques have been applied to detect the position of the MPP on the power-voltage curve of the PV array in less search steps.

A golden section search algorithm was employed in [43], where the MPPT process is performed by iteratively narrowing the range of the PV output voltage values where the MPP resides. For each search range $[V_{\min}, V_{\max}]$, the output power of the PV source is measured at two operating points of the PV source, where the values of the PV source output voltage (*i.e.*, parameter V in Figures 1, 2, and 5(b)), V_1 and V_2, respectively, are given by

$$V_1 = V_{\max} - r \cdot (V_{\max} - V_{\min}), \tag{12}$$

$$V_2 = V_{\min} + r \cdot (V_{\max} - V_{\min}). \tag{13}$$

where $r = 0.618$ to place V_1 and V_2 symmetrically within $[V_{\min}, V_{\max}]$ and, also, for placing V_2 at a position with a ratio of distances from V_1 and $V_{\max}$, respectively, which is equal to the ratio of distances of V_1 from $V_{\min}$ and $V_{\max}$, respectively, while initially it holds that $V_{\min} = 0$ and $V_{\max} = V_{oc}$.

Then, the PV module/array output power is measured at V_1 and V_2. If the output power at V_1 is higher than that at V_2, then it is set that $V_{\max} = V_2$; else, it is set that $V_{\min} = V_1$. This

process is repeated until the distance between $V_{\min}$ and $V_{\max}$ is smaller than a predefined value.

In [44], a multi-stage MPPT process was presented, comprised of a combination of the P&O, golden section search, and InC algorithms. A flowchart of this process, which is based on the method proposed in [44], is depicted in Figure 9. Initially, the P&O algorithm is applied with a large perturbation step to converge quickly close to the MPP. Then, the golden section search algorithm is applied for accurately and quickly detecting the MPP; finally, the InC algorithm is executed for ensuring operation at the MPP at steady state, as well as for triggering the initiation of a new search process in case that a large deviation from the MPP is detected (*i.e.*, when $\partial P/\partial V > \varepsilon$, where ε is a preset threshold) due to changing environmental conditions.

An iterative approach, where the search window is progressively modified, is also performed in the linear iteration algorithm, as presented in [45]. However, in that case, the new search range at each iteration of the algorithm is calculated based on the power slope of the abscissa on the power-voltage characteristic of the point that is defined as the intersection of the tangent lines at $V_{\min}$ and $V_{\max}$ (*i.e.*, point Q in Figure 10, which is based on the procedure proposed in [45]). If the gradient at point Q is positive, then Q is set as the new lower limit of the search range; else, it will be the upper limit.

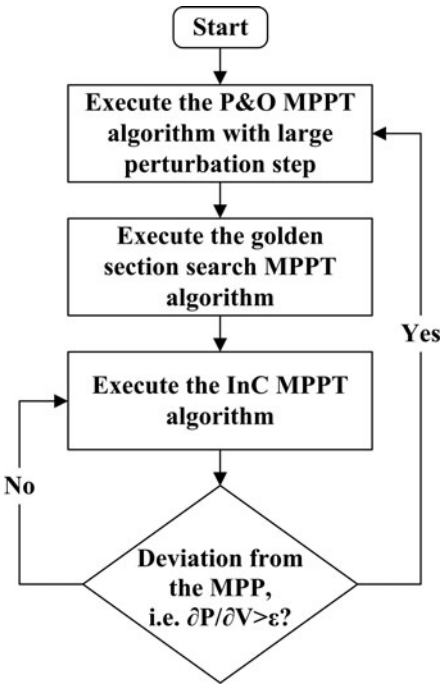

FIGURE 9. A flow-chart of a multi-stage MPPT process, comprising the P&O, golden section search and InC algorithms, based on the procedure proposed in R. Shao et al., 29th Annual IEEE APEC, p. 676, 2014.

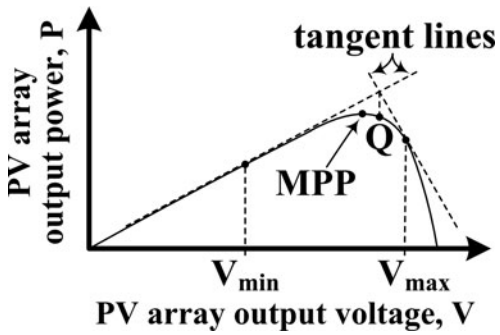

FIGURE 10. The operating principle of the linear iteration process, using numerical optimization algorithm for MPPT, based on the procedure proposed in W. Xu et al., IEEE Trans. AS-24(5), 2014.

In the parabolic prediction MPPT algorithm [46], the power-voltage curve of the PV source, $P(V)$, is approximated by a parabolic curve, $Q(V)$, which is given by

$$Q(V) = P(V_o)\frac{(V - V_1)\cdot(V - V_2)}{\Delta V_{01}\cdot\Delta V_{02}} + P(V_1)\frac{(V - V_0)\cdot(V - V_2)}{\Delta V_{10}\cdot\Delta V_{12}} + P(V_2)\frac{(V - V_0)\cdot(V - V_1)}{\Delta V_{20}\cdot\Delta V_{21}}, \quad (14)$$

where V_i is the output voltage of the PV source (*i.e.*, parameter V in Figures 1, 2, and 5(b)) at the ith operating point; $\Delta V_{ij} = V_i - V_j$ $(i, j = 0, 1, 2)$.

During the execution of the MPPT process, the output power and voltage of the PV source are measured at three operating points (*e.g.*, A, B, and C in Figure 11, which is

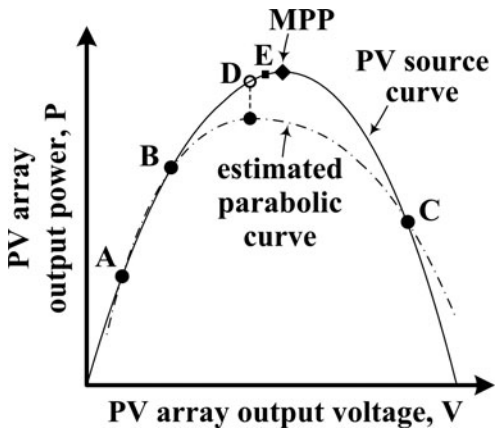

FIGURE 11. The parabolic prediction MPPT algorithm based on the procedure proposed in F.-S. Pai et al., IEEE Trans. SE-2(1), p. 60, 2011.

based on the procedure proposed in [46]), and the corresponding parabolic curve is calculated using Eq. (14). The resulting parabolic curve is used to estimate the MPP location (*i.e.*, D in Figure 11), which deviates from the real MPP of the PV source depicted in Figure 11. Similarly, a new parabolic curve is calculated at the next iteration of the algorithm using the three operating points that produce the highest values of power (*i.e.*, B, D, and C in Figure 11), resulting in operation at E, which is closer to the MPP than point D is. This process is repeated until the power deviation of the MPPs calculated at two successive iterations is less than a predefined level.

Although effective in deriving the MPP of the PV source, these techniques exhibit higher implementation complexity compared to the simpler algorithms, such as the P&O and InC MPPT methods.

3.8. Ripple Correlation Control (RCC) MPPT

To avoid employing a derivative for performing the MPPT process, the gradient of the power-voltage curve, $\frac{\partial P}{\partial V}$, employed in the P&O technique for detecting the direction toward which the MPP resides, is replaced in the RCC MPPT method by the following correlation function [47]:

$$c(t) = \frac{\partial P}{\partial t} \cdot \frac{\partial V}{\partial t}. \tag{15}$$

In the case when a DC/DC converter is used to interface the PV generated energy to the load, then the duty cycle of the power converter at time t, $d(t)$, is adjusted according to the following control law:

$$d(t) = k \cdot \int_0^t sign(c_{lp}(\tau))d\tau, \tag{16}$$

where k is a constant, and $c_{lp}(t)$ is the result of low-pass filtering correlation function $c(t)$ given by Eq. (15).

To simplify the hardware implementation of the MPPT system, the values of $\frac{\partial P}{\partial t}$ and $\frac{\partial V}{\partial t}$ in Eq. (15) are calculated by measuring the AC disturbances (*i.e.*, ripples) at the operating point of the PV source, which are due to the high-frequency switching operation of the power converter. The derivatives are measured using high-pass filters with a cut-off frequency higher than the ripple frequency (*i.e.*, switching frequency) [48]. In [49], the PWM dithering technique is applied for increasing the resolution of the power converter PWM control signal. The resulting ripple in the output current and voltage of the PV source, which is due to the dithering process, is then exploited for applying the RCC MPPT method.

Targeting to increase the accuracy of the MPPT, a variation of the RCC method was proposed in [50], where as soon as a deviation in the phase displacement of the PV voltage and current is observed, that indicates that the peak of the current ripple of the PV source has reached the MPP. Then the DC component of the PV source output current is regulated at the value of the detected MPP.

The RCC MPPT method exhibits a fast response, but its operation is based on the existence of switching ripples, which might be undesirable during the operation of power converters. Also, the performance of this MPPT technique is affected by the accuracy of the measurements of correlation function $c(t)$.

3.9. Extremum Seeking Control (ESC) MPPT

ESC is a self-optimizing control strategy [51] that operates based on a similar principle with RCC MPPT; the difference is that instead of using the high-frequency switching ripple, which is inherent in the power converter, ESC is based on the injection of a sinusoidal perturbation [52–55]. The block diagram of an ESC scheme based on the method presented in [55] is shown in Figure 12. Control signal $d(t)$ corresponds to the duty cycle of the power converter. PV module/array

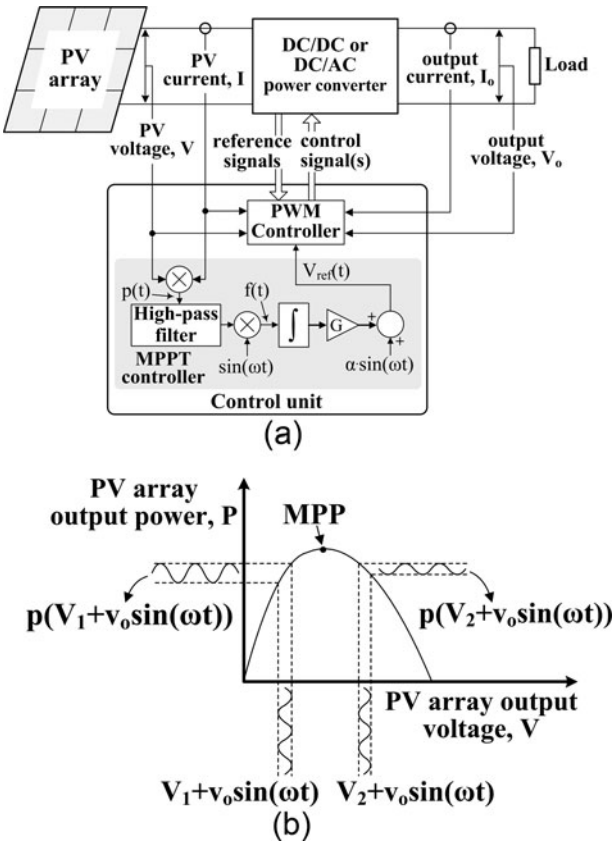

FIGURE 12. Extremum Seeking Control-based PV MPPT based on the method presented in H. Malek et al., 29th Annual IEEE APEC, p. 1793, 2014: (a) a block diagram of the MPPT controller and (b) the resulting operating points on the power-voltage curve of the PV source.

output power $p(t)$ is passed through a high-pass filter and demodulated. The resulting signal (*i.e.*, $f(t)$ in Figure 12(a)) has a positive sign in the case when the operating point is on the left side of the power-voltage curve in Figure 2(a), since the perturbation and PV source output power signals are in phase in that case; otherwise, its sign is negative (Figure 12(b)). The control signal is produced by integrating $f(t)$ and then adding the perturbation $\alpha \cdot \sin(\omega t)$.

The ESC-based MPPT process has the disadvantage that for its implementation in a PV power processing system, the development of a relatively complex control circuit is required.

3.10. MPPT Based on Sliding-mode Control

In sliding-mode control MPPT, the output voltage of the PV source and the current of the power converter inductor comprise a set of state variables. A switching surface is defined using these state variables, as follows [56]:

$$S(v, i_{in}) = c_1 \cdot i_{in} - c_2 \cdot v + V_{ref}, \tag{17}$$

where i_{in} is the current of the power converter inductor, c_1 and c_2 are positive constants, and V_{ref} is an adjustable control signal.

A block diagram of a sliding-mode control MPPT system based on the method proposed in [56] is illustrated in Figure 13. During operation, the value of $S(v, i_{in})$ is evaluated; in the case when $S(v, i_{in}) > 0$, transistor T_1 is turned off, and the energy is transferred toward the load; else, T_1 is turned on such that energy is stored in input inductor L. The value of V_{ref} is adjusted by a P&O MPPT algorithm such that the PV source operates at the MPP. To accelerate the convergence to the MPP, the values of c_1 and c_2 in Eq. (17) are selected such that the operating points $[v,\ i_{in}]$, which are defined by $S(v, i_{in}) = 0$, match the locus of the PV source MPPs under various solar irradiation conditions with the minimum possible deviation. Thus, for the implementation of this MPPT technique, the knowledge of the PV source operational characteristics is required, which is a disadvantage.

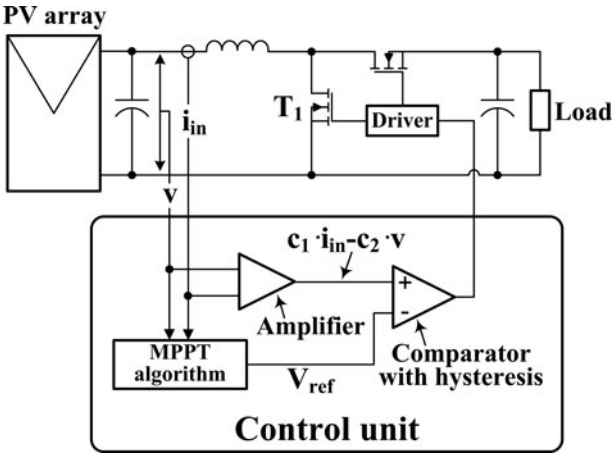

FIGURE 13. A block diagram of an MPPT system employing sliding-mode control based on the method proposed in Y. Levron et al., IEEE Trans. CSI-60(3), p. 724, 2013.

As demonstrated in [56], compared to the MPPT based on the PWM principle, sliding-mode control MPPT provides a faster response under dynamic conditions.

3.11. Comparison of MPPT Methods for Uniform Solar Irradiation Conditions

A comparison of the operational characteristics of the MPPT methods for uniform solar irradiation conditions is presented in Table 2. As analyzed in Sections 3.2 and 3.3, the P&O and InC methods are characterized by implementation simplicity and exhibit equivalent static and dynamic performance. Although their operation can be affected by external disturbances (*e.g.*, system noise, short-term or rapidly changing meteorological conditions, etc.), they are able to recover and move toward the correct direction, where the MPP resides, as soon as the disturbance has been diminished. The constant-voltage, constant-current model-based MPPT and artificial intelligence-based methods are more robust compared to the P&O and InC methods, since they are less affected by external disturbances. However, their efficiency is lower due to the periodic interruption of the PV source for measuring the open-circuit voltage/short-circuit current of the PV source. The resulting efficiency is further reduced in the case that accurate knowledge of the PV source operational parameters, which is required for their implementation, is not available. The single-sensor MPPT approach comprises a P&O MPPT method, thus exhibiting equivalent robustness to external disturbances with the P&O approach, but its efficiency is lower due to the deviation of the power converter operation, which is predicted using a theoretical model, from the actual performance obtained under practical operating conditions due to the tolerance of the electric/electronic components values, circuit parasitics, etc.

In numerical optimization MPPT algorithms (except the multi-stage and parabolic prediction MPPT methods), a scan process is periodically repeated to detect possible changes of the MPP position, which results in efficiency reduction due to the associated power loss until convergence to the MPP has been achieved. The numerical optimization MPPT algorithms do not require significant system knowledge for their application, but their implementation complexity is higher than that of the P&O and InC methods. Among the numerical optimization MPPT algorithms, the multi-stage and parabolic prediction MPPT methods exhibit similar performance with the P&O

MPPT method	Sampling rate	Complexity	Robustness		Efficiency	Sampled parameters	System or expert knowledge required	Constant-power operation
			To external disturbances	To aging of the PV modules				
Constant voltage/constant current	High	Very low	Very high	Low	Low	PV voltage or current	High	Difficult
P&O	Low	Low	High	High	High	PV voltage and current	Low	Easy
InC	Low	Low	High	High	High	PV voltage and current	Low	Easy
Model-based	Low	High	Very high	Low	Low	PV voltage and current	Very high	Easy
Artificial intelligence-based	Low	Very high	Very high	ANN: low	Low	Irradiation and temperature	Very high	Difficult
				Fuzzy logic: high		PV current and voltage		Easy
Single-sensor	Low	Low	High	High	Low	PV voltage	High	Difficult
Numerical optimization	Multi-stage and parabolic prediction: low Others: high	High	Multi-stage and parabolic prediction: high Others: low	High	Multi-stage and parabolic prediction: high Others: low	PV voltage and current	Low	Easy
RCC	Low	High	Low	High	High	PV voltage and current	High	Easy
ESC	Low	High	High	High	High	PV voltage and current	High	Easy
Sliding-mode control	Low	Low	Very high	Low	Very high	PV voltage and current	High	Easy

TABLE 2. Comparison of operational characteristics of MPPT methods for uniform solar irradiation conditions

and InC methods. The robustness of the remaining numerical optimization MPPT algorithms is affected by external disturbances, since they are not able to recover from possible error estimations, which are performed due to the decisions taken during each iteration until the next scan process is re-initiated.

Due to the exploitation of the inherent, low-amplitude switching ripples of the power converter for performing the MPPT process, the robustness of the RCC MPPT technique may easily be affected by the impact of external disturbances on the accuracy of calculating the PV power-voltage correlation function. Additionally, appropriate co-design of the power converter and MPPT control system is required for implementation of the RCC MPPT method, thus requiring system knowledge to be available. The control circuit complexity of the RCC and ESC MPPT techniques is relatively high. A better robustness to external disturbances is obtained using the ESC method compared to the RCC-based MPPT approach, since its operation is based on the injection of perturbation signals, rather than using the inherent, low-amplitude switching ripples of the power converter. However, detailed knowledge of the PV system operational characteristics is still required by the ESC method for tuning the operational parameters of the MPPT control loop. Both the RCC and ESC MPPT methods operate by employing a continuously operating feedback loop; thus, their efficiency is not affected by periodic disruptions of the PV source operation.

The MPPT method based on sliding-mode control requires knowledge of the PV source operational characteristics. Since the PWM generator is replaced by a sliding-mode controller and a P&O MPPT process is also performed during its execution, the complexity of the corresponding control circuit is similar to that of the P&O MPPT process. However, better efficiency and robustness to external disturbances may be obtained under dynamic conditions compared to the PWM-based P&O MPPT method due to the faster response of the sliding-mode MPPT controller.

The constant-voltage/constant-current, model-based MPPT and ANN-based and sliding-mode control methods operate based on knowledge of the PV source electrical characteristics. Thus, their accuracy is highly affected by the PV modules aging, unless the drift of the PV source operational characteristics with time is compensated through a suitable model, which, however, is difficult to derive and would increase the complexity of the control unit.

In contrast to the rest of the MPP methods that perform the MPPT process through a continuously operating feedback loop, the periodic re-initialization of the MPPT process required in the constant-voltage, constant-current, and numerical optimization techniques (except the multi-stage and parabolic prediction MPPT methods) imposes the need to apply a high sampling rate to be able to quickly detect the MPP position changes.

All MPPT methods presented in this section are suitable to accommodate a constant-power-mode control scheme [5], except the constant-voltage, constant-current, ANN-based, and single-sensor MPPT techniques, since, due to the types of sampled parameters, which are employed in these methods, they do not comprise the sensors required to facilitate the measurement of the PV output power.

4. MPPT METHODS FOR PV ARRAYS OPERATING UNDER NON-UNIFORM SOLAR IRRADIATION CONDITIONS

When the individual modules of the PV array receive unequal amounts of solar irradiation, the power-voltage characteristic of the PV source exhibits multiple MPPs, the positions of which change continuously under the influence of the stochastically varying meteorological conditions. In such a case, the target of an MPPT process is to derive, among the individual local MPPs of the PV source, the global MPP where the overall power production of the PV array is maximized. Multiple alternative techniques have been developed in the past that are suited for application under non-uniform solar irradiation conditions (see Figure 4), and their operating principles are described and compared in what follows.

4.1. PV Array Reconfiguration

To increase the power that is supplied to a constant resistive load by a PV array operating under partial shading conditions, the use of a matrix of power switches was proposed in [57]. Using this matrix, the connections between the PV cells/modules are dynamically modified such that the PV strings comprise PV cells/modules operating under similar solar irradiation conditions.

The PV array reconfiguration method has the disadvantages of higher implementation complexity and cost due to the high number of power switches required, but it increases the energy production of the PV array. According to [6], since the power-voltage curve of the PV array after reconfiguration may still exhibit local MPPs, a power converter executing one of the global MPPT algorithms presented in the following should be connected at the output of the PV source to maximize the generated power.

4.2. Evolutionary MPPT Algorithms

In this class of MPPT techniques, the MPPT process is treated as an optimization problem, where the optimal value of the decision variable is calculated in real time, such that the objective function, which corresponds to the power-voltage curve of the PV source, is maximized. Thus, various alternative evolutionary optimization algorithms, in some cases inspired from biological and natural processes, have been applied for that purpose. A generalized flowchart of an evolutionary algorithm for implementing an MPPT process is shown in Figure 14.

Initially, the designer specifies the values of the optimization algorithm operational parameters that define the speed and accuracy of convergence to the global optimum solution. During the execution of the optimization/MPPT process, multiple sets of values of the decision variable are produced in a way defined by the operating principle of the specific optimization algorithm, which has been employed. By appropriately controlling the power converter, the PV source is set to operate at the alternative operating points corresponding to each of these

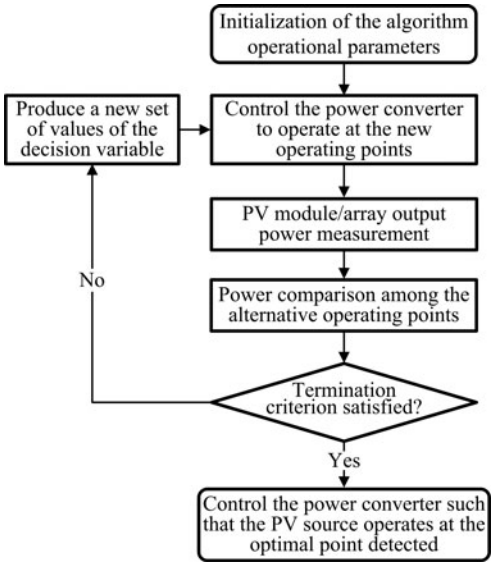

FIGURE 14. Generalized flowchart of an evolutionary algorithm for implementing an MPPT process.

sets. At each operating point, the power generated by the PV source is measured (*i.e.*, the objective function of the optimization problem is evaluated) and compared to the power produced at other operating points. This process is iteratively repeated, until a convergence criterion has been satisfied, which indicates that the position of the global MPP on the power-voltage curve has been derived. Then the PV source is set to operate at the optimal operating point derived during the execution of the optimization algorithm.

Alternative evolutionary algorithms, as well as their variations, have been applied for performing the MPPT process, such as GAs [58], differential evolution (DE) [59], particle swarm optimization (PSO) [60–62], and the firefly algorithm (FA) [63]. A hybrid MPPT technique, which is a combination of the P&O and PSO algorithms, was proposed in [64]. The decision variable employed during the application of the above algorithms is either the duty cycle of the power converter or the reference voltage of the PI regulator, which controls the power converter DC input voltage.

The evolutionary MPPT algorithms exhibit algorithmic complexity, thus necessitating the use of microcontrollers or DSP units for their implementation. Also, since random numbers are employed during the execution of the evolutionary MPPT algorithms, it cannot be mathematically guaranteed that they will converge to the global MPP under any partial shading conditions.

4.3. MPPT Methods Based on Numerical Optimization Algorithms

These algorithms employ numerical methods that are suitable for deriving the maximum of an objective function without requiring the calculation of derivatives of the objective function. Thus, due to their inherent computational simplicity, they can effectively be implemented into a microcontroller or DSP device within the control unit of the PV energy management system.

In the dividing rectangles (DIRECT) algorithm [65], individual intervals within the output voltage range of the PV source are iteratively explored for detecting the position of the global MPP. Each such interval is divided into three subintervals of equal range. Among them, the potentially optimal interval is defined as the jth interval $[\alpha_j, b_j]$ for which there exists a value $K > 0$ satisfying the following inequalities for each value of i ($i = 1, \ldots, 3$):

$$p(c_j) + K\frac{b_j - \alpha_j}{2} \geq p(c_i) + K\frac{b_i - \alpha_i}{2}, \tag{18}$$

$$p(c_j) + K\frac{b_j - \alpha_j}{2} \geq p_{\max} + \varepsilon\,|p_{\max}|\,, \tag{19}$$

where c_j and c_i are the midpoints of intervals j and i, respectively; α_i and b_i are the end points of the ith interval; $\varepsilon > 0$ is a constant; and $p_{\max}$ is the power at the currently detected MPP.

Only potentially optimal intervals are selected for reapplying the same dividing process until the global MPP is detected [66]. However, it is not guaranteed that under any partial shading conditions the DIRECT MPPT algorithm will be able to achieve convergence to the global MPP with a fewer number of steps than an exhaustive-search procedure, which sweeps the entire power-voltage curve of the PV source.

In [67], a sequence of Fibonacci search numbers (*i.e.*, $F_0 - F_n$ $[n \geq 0]$) is produced for performing the MPPT process under partial shading conditions, as follows:

$$F_0 = 0, \quad F_1 = 1, \quad F_n = F_{n-2} + F_{n-1} (n \geq 2). \tag{20}$$

In the ith iteration of the search process, the control signal of a boost-type DC/DC converter connected to the PV source is adjusted to values c_1^i and c_2^i ($c_1^i < c_2^i$) that lie within the search interval $[c_3^i, c_4^i]$. Distance α_i between c_1^i, c_3^i and c_2^i, c_4^i, as well as the distance b_i between c_1^i, c_2^i, are given by

$$\begin{aligned} \alpha_i &= F_{n+1}, \qquad b_i = F_n. \\ \alpha_{i+1} &= F_n, \qquad b_{i+1} = F_{n-1}. \end{aligned} \tag{21}$$

The next search interval is decided by comparing the PV output power at c_1^i and c_2^i as follows: if $p(c_1^i) < p(c_2^i)$, then $c_3^{i+1} = c_1^i$ and $c_4^{i+1} = c_4^i$; else, $c_3^{i+1} = c_3^i$ and $c_4^{i+1} = c_2^i$. This search process is continued until the variable n of F_n is reduced to zero or the distances between c_3^i, c_4^i and $p(c_3^i)$, $p(c_4^i)$, respectively, drop below predefined thresholds. The MPPT algorithm based on the Fibonacci sequence does not guarantee convergence to the global MPP.

4.4. Stochastic and Chaos-based MPPT Algorithms

The random search method (RSM) was applied in [68] for deriving the global MPP of a PV array with partial shading. Using this approach, the duty cycle of a DC/DC power converter is iteratively modified using random numbers so it progressively moves toward values that operate the PV source at points providing a higher output power.

The chaotic-search global MPPT process presented in [69] is based on two recursive functions (*i.e.*, dual carrier) to perform iterative fragmentations of the PV array power-voltage characteristic. For that purpose, sequences of numbers are generated through the use of appropriate functions that correspond to alternative operating points on the power-voltage characteristic of the PV array. By measuring the power generated by the PV array at these positions, the global MPP is detected. In [70], the global MPPT process for flexible PV modules that also exhibit local MPPs on their power-voltage curves was

performed using a combination of the dual-carrier (*i.e.*, using two recursive functions) chaotic-search and PSO algorithms.

Due to their operational complexity, a microcontroller- or DSP-based control unit is required for executing these global MPPT algorithms.

4.5. Distributed MPPT (DMPPT)

In case that the PV source, which is connected to the power converter of the PV energy production system shown in Figure 1, comprises strings of series-connected PV modules, then a bypass diode is connected in anti-parallel with each PV module to conduct the string current in the case of partial shading conditions. In contrast to this design approach, in DMPPT architectures, a separate DC/DC power converter is connected at the output of each PV module of the PV array.

In the current equalization DMPPT topology, the DC/DC converter connected at the output of each PV module is power-supplied by the DC bus of the PV string. A diagram of this topology based on the architecture proposed in [71] is depicted in Figure 15. Under partial shading conditions, the *n*th PV module produces a current equal to $i_{pv,n}$, and the corresponding DC/DC converter is controlled to supply an additional current that is equal to $i_s - i_{pv,n}$ such that the total string current is equal to i_s. At the same time, the output voltage of each PV module is regulated such that operation at its MPP is ensured [72]. The position of the MPP is different for each PV module, depending on the geometry of the shading pattern on the PV array. Each DC/DC converter is required to supply only the equalization current, thus operating at a low power level with relatively low power losses.

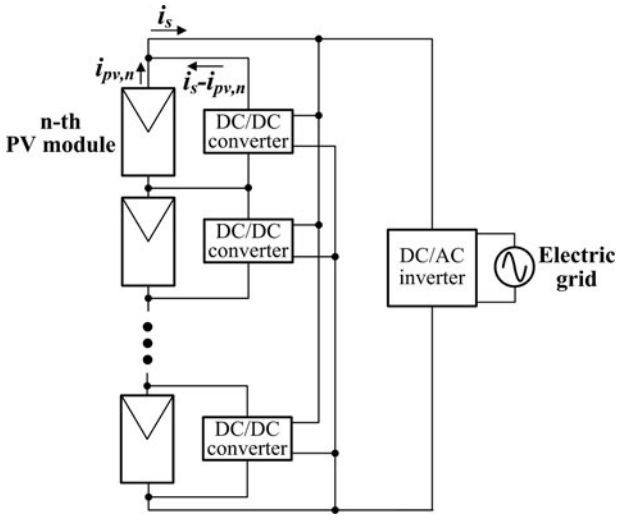

FIGURE 15. A diagram of the current equalization Distributed MPPT topology based on the architecture proposed in P. Sharma et al., 38th IEEE PVSC, p. 1411, 2012.

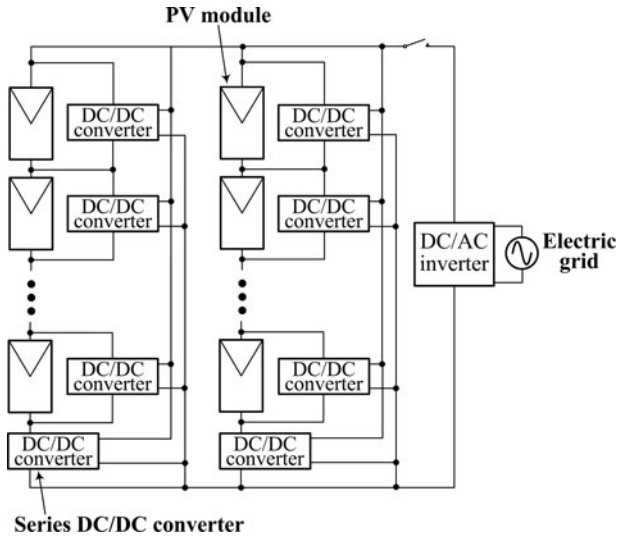

FIGURE 16. A diagram of the shunt-series compensation Distributed MPPT topology based on the architecture proposed in P. Sharma et al., IEEE J. Photovolt.-4(4), p. 1128, 2014.

To enable multiple strings, each employing the current equalization topology described above, to be connected in parallel without forcing their PV modules to operate away from their MPPs, the current equalization topology presented above has been extended to the shunt-series compensation topology. A diagram of this topology based on the architecture proposed in [73] is shown in Figure 16. In this architecture, a current-compensating DC/DC converter is connected in parallel with each PV module, and a voltage-compensating DC/DC converter is connected in series with each PV string, which balances the deviation of the total voltage produced by parallel-connected strings, thus enabling the individual PV modules to operate at their own MPPs.

An alternative DMPPT topology based on the methods presented in [74–76] is illustrated in Figure 17. In this case, the PV strings are formed by connecting in series the outputs of the DC/DC converters, which are connected at the output of each PV module. Each DC/DC converter processes the entire power generated by the corresponding PV module and executes the MPPT process for that individual PV module.

Alternative DMPPT control schemes based on the methods presented in [75] are illustrated in Figure 18. The MPPT process may be performed by either executing the MPPT process (*e.g.*, P&O) at each DC/DC converter separately or by measuring the total power of the DC bus and then sending the appropriate control signal to each DC/DC converter. In the latter case, the power losses of the individual power converters are also taken into account in the MPPT process.

The diagram of an architecture employing a triggering circuit in parallel with each PV module of the PV string, to-

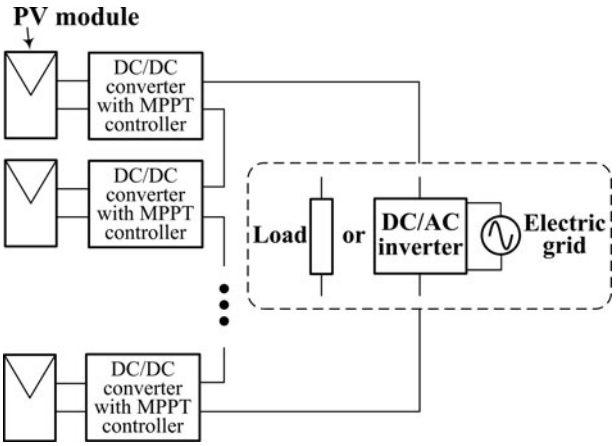

FIGURE 17. Distributed MPPT topology where the outputs of the DC/DC converters are connected in series, based on the methods presented in P. Sharma et al., IEEE Trans. PEL-29(9), p. 4684, 2014, C.A. Ramos-Paja et al., ICCEP, p. 48, 2013 and F. Scarpetta et al., 38th IEEE IECON, p. 5708, 2012.

gether with an energy-recovery unit across the PV string, based on the design method proposed in [77] is depicted in Figure 19. The triggering circuit measures the voltage developed across the bypass diode. When this voltage exhibits a low negative value, indicating that the corresponding bypass diode conducts current, and thus a partial shading condition has evolved, the energy-recovery circuit is activated to bypass that

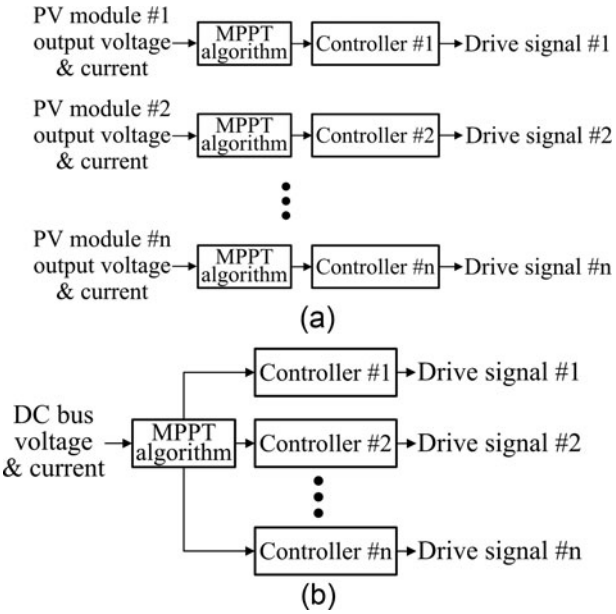

FIGURE 18. Alternative Distributed MPPT control schemes based on the methods presented in C.A. Ramos-Paja et al., ICCEP, p. 48, 2013: (a) MPPT at the DC/DC converter level and (b) centralized MPPT.

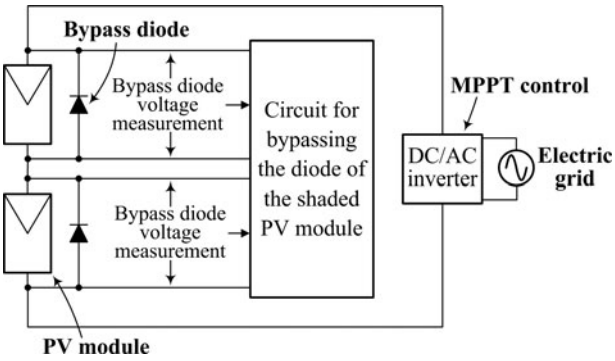

FIGURE 19. The diagram of a Distributed MPPT topology with an energy recovery circuit in parallel with each PV module based on the design method proposed in M.Z. Ramli et al., IEEE Trans. PEL-29(12), p. 6458, 2014.

diode. In this case, part of the current of the less shaded PV modules is diverted into the energy-recovery circuit, thus maintaining the current of all PV modules at the same value without requiring the activation of the bypass diodes of the shaded PV modules. The resulting power-voltage curve of the PV string exhibits a single MPP, without local MPPs, which is tracked by the MPPT unit of a central DC/AC inverter.

The DMPPT approach has the advantage that the total available MPP power of the PV array is increased. However, compared to the PV system topology where a single central power converter is used for processing the energy generated by the entire PV array, the implementation complexity of the DMPPT architectures is higher due to the requirement to install a separate DC/DC converter at each PV module of the PV source.

4.6. Other Global MPPT Methods

Scanning of the power-voltage curve was performed in [78] by varying the duty cycle of a DC/DC power converter (see Figure 1) to detect the position of the global MPP either during initial operation or during varying atmospheric conditions. A fuzzy logic-based MPPT process is then applied to track short-term changes of the global MPP. A similar two-stage process was applied in [79]. With a goal to restrict the voltage range to be scanned, thus reducing the time required to accomplish the scan process and the associated power loss, the voltage windows explored during the scanning process were continuously updated in [80] based on the geometry of the power-voltage curve of the PV array under partial shading conditions. The calculation of the voltage windows is performed using the value of the open-circuit voltage of the PV modules comprising the PV source, which must be known prior to the application of this global MPPT method.

In [4], a buck-type DC/DC converter is controlled so that it operates as an adjustable constant-power load of the PV array,

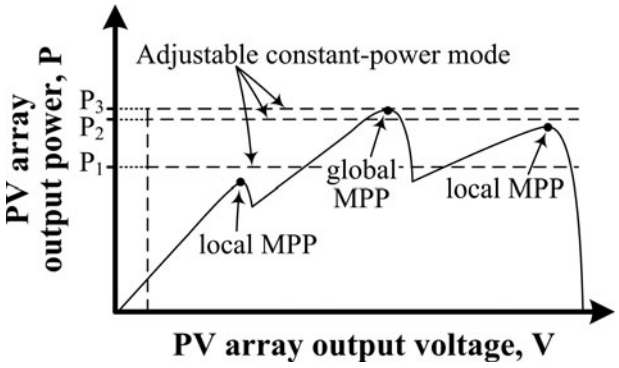

FIGURE 20. A diagram of the operation in adjustable constant-power mode for avoiding convergence to local MPPs during the global MPPT process based on the method proposed in E. Koutroulis et al., IEEE J. Photovolt.-2(2), p. 184, 2012.

thus avoiding operation at local MPPs of the PV power-voltage curve. A diagram of the operation in adjustable constant-power mode for avoiding convergence to local MPPs during the global MPPT process based on the method proposed in [4] is depicted in Figure 20. Although the periodic scanning of the PV source power-voltage curve is also performed by this global MPPT method, the number of search steps that must be executed for detecting the position of the global MPP is lower than those required by an exhaustive-search process. Additionally, this technique does not require knowledge of either the PV source configuration or the individual PV modules electrical characteristics.

A thermal imaging camera was used in [81] for acquiring thermal images of a PV array containing partially shaded PV modules. These images are then analyzed using a model of the PV array to estimate the voltage corresponding to the global MPP. Although the implementation cost of this MPPT method is relatively high due to the thermal imaging camera employed, the operation of the PV system is not disturbed for tracking different operating points during the global MPP detection process.

In [82], the global MPPT process was based on the assumption that the local MPPs occur at voltages that are an integer multiple of about 0.8 V_{oc}, where V_{oc} is the open-circuit voltage of the PV modules that comprise the PV source. Thus, the PV array voltage was modified at steps of 0.8 V_{oc}, and at each step, the position of the local MPP was derived using an InC MPPT algorithm. The power levels of the local MPPs were compared, and among them, the global MPP corresponds to that providing the maximum amount of power. The InC MPPT algorithm was also used to maintain operation at the previously detected global MPP until a variation of incident solar irradiation is detected, which ignites a new execution of the global MPPT process. The application of this MPPT technique requires knowledge of the value of V_{oc}, as well as its sensitivity to the ambient temperature and solar irradiation.

An ANN was trained in [83] for producing the location of the global MPP of a PV array under various solar irradiation conditions. The ANN training was performed by using the power-voltage curves of the PV source, produced by using the single- or two-diode model of the PV modules. Thus, this MPPT method requires knowledge of the PV source operational characteristics to perform the ANN training process. During the global MPP process, measurements of incident solar irradiation on each PV module of the PV array were input in the off-line trained ANN, which then produces an estimation of the approximate position of the global MPP. This information is used as an initial operating point by a P&O MPPT algorithm for deriving the true global MPP.

In [84], the current-voltage curve of the PV source was initially traced by disconnecting it from the power converter and connecting it to a parallel RC circuit containing a discharged capacitor. This action causes the PV source voltage to sweep in the range of 0–V_{oc}. The current and voltage measurements acquired during that tracing process were used to move the PV source operating point to a region close to the global MPP. Then a P&O algorithm was applied for converging to the global MPP. This technique has the disadvantage that during the execution of the current-voltage curve tracing process, the PV source power is not transferred to the PV system load.

In an alternative MPPT method, the total output voltage range of the PV source (*i.e.*, 0–V_{oc}) is divided into intervals, and the corresponding output power is measured at each interval [85]. The P&O MPPT method with variable step size (*i.e.*, reducing the step size as the MPP is approached) is then applied for tracking the global MPP at the particular interval that provided the highest power measurement. The number of intervals is selected to be higher than the number of PV modules connected in series in the PV source, thus requiring the knowledge of the PV source operational characteristics.

The output voltage of each PV module of the PV string was measured in [86] for calculating the number q of different levels of solar irradiation G_j ($G_1 < G_2 < ... < G_q$), which are received by the PV string and the corresponding number of PV modules receiving each such level M_j ($j = 1, \ldots, q$). A P&O MPPT process is then applied at the entire PV string, which is initiated at the open-circuit voltage of the PV string V_{oc} as well as at each of the distinct PV string voltage levels defined by the following equation for $j = 1, \ldots, q-1$:

$$V_{pv,j} = 0.85 \cdot \left(1 - \frac{\sum_{i=1}^{j} M_i}{N} \right) \cdot V_{oc}, \tag{22}$$

MPPT method	Sampling rate	Complexity	Robustness		Efficiency	Sampled parameters	System or expert knowledge	Constant-power operation
			To external disturbances	To aging of the PV modules				
PV array reconfiguration	High	High	Low	Low	High	PV voltage and current	High	Very difficult
Evolutionary MPPT algorithms	High	High	Low	High	Low	PV voltage and current	Low	Easy
Numerical optimization	High	Low	Low	High	Low	PV voltage and current	Low	Easy
Stochastic/chaos-based algorithms	High	High	Low	High	Low	PV voltage and current	Low	Easy
DMPPT	Low	Very high	High	Depends on the type of MPPT method employed	Very high	PV voltage and current	High	Easy
Other global MPPT methods	High	Method-dependent	Method-dependent	Method-dependent	Low	PV voltage and current	High in most cases	Easy in most cases

TABLE 3. Comparison of operational characteristics of global MPPT methods for non-uniform solar irradiation conditions

where N is the total number of PV modules of the PV string.

By comparing the power produced at the individual MPPs tracked by the P&O algorithm, the position of the global MPP is derived. However, the number of voltage sensors and accompanying signal-conditioning circuits are significantly high when applying this technique in PV sources composed of strings with a high number of PV modules, thus increasing the complexity and cost of the control unit.

In [87], the ESC MPPT method is sequentially applied at individual segments of the voltage range of the PV array to detect the positions of local MPPs. Among them, the local MPP where the maximum power is produced corresponds to the global MPP. A similar process was also applied in [88], but in this case, the segments that do not contain the global MPP are identified using information about the gradient of the power-voltage curve. By this technique, convergence to the (local) MPP of these segments is avoided, thus speeding up the global MPP detection process. In the ESC-based global MPPT method, the individual segments of the PV source output voltage range are selected using the values of the PV modules electrical characteristics, which must be known when developing the corresponding MPPT system. Additionally, the complexity of the control circuit, which implements the ESC-based global MPPT technique, is relatively high.

4.7. Comparison of Global MPPT Methods for Non-uniform Solar Irradiation Conditions

The global MPPT methods for non-uniform solar irradiation conditions, previously described, are compared in terms of their operational characteristics in Table 3. With the exception of the DMPPT techniques, the remaining global MPPT algorithms presented in this section require periodic re-initialization of their execution. This is indispensable to be able to detect a possible displacement of the global MPP position due to a change of either the meteorological conditions or the shading pattern on the surface of the PV array (*e.g.*, change of the shadow shape due to sun movement etc.). This results in power loss until the MPPT algorithm convergences to the new global MPP and also imposes the need of a high sampling rate to be able to quickly detect the global MPP changes. The application of the PV array reconfiguration method requires knowledge of the configuration of the PV source but provides a high efficiency, since the PV system is able to produce more power than that at the global MPP without reconfiguration.

Due to their inherent randomness, the evolutionary, stochastic, and chaos-based MPPT algorithms do not guarantee convergence to the global MPP under any partial shading conditions. Thus, they exhibit a lower efficiency. However, they have the advantage of not requiring detailed knowledge of the PV system operational characteristics. The global MPPT methods based on numerical optimization algorithms either do not guarantee convergence to the global MPP or convergence can be accomplished after a large number of search steps, both resulting in a reduction of the PV-generated energy. The robustness of the PV array reconfiguration, evolutionary, stochastic, chaos-based, and numerical optimization-based MPPT algorithms may easily be degraded by external disturbances affecting the correctness of the decisions taken during the global

MPPT process with respect to the direction toward which the global MPP resides. In such a case, possible wrong estimations may only be recovered at the next re-execution of the corresponding MPPT algorithm. The DMPPT techniques require knowledge of the PV source configuration, but they are able to extract the maximum possible energy from the PV source at the cost of a significantly higher hardware complexity. Most of the other global MPPT algorithms, presented in Section 4.6, require knowledge of the operational characteristics of the PV source. Also, since a search process is applied periodically during their execution to detect possible changes of the global MPP position (*e.g.*, due to a change of meteorological conditions), the power produced by the PV source is reduced, and also a high sampling rate is required. Their performance in terms of the remaining metrics considered in Table 3 depends on the specific technique applied in each case.

The evolutionary, stochastic, chaos-based, and numerical optimization-based MPPT algorithm methods, as well as some of the global MPPT approaches presented in Section 4.6, do not operate by using information about the electrical characteristics of the PV source, so their accuracy is not affected by the PV modules aging. The robustness of DMPPT architectures to the PV modules aging depends on the type of the method employed for performing the MPPT process.

Among the global MPPT methods presented, the PV array reconfiguration approach is the least suitable for operation in combination with a constant-power-mode controller [5] due to the low power adjustment resolution achieved by controlling the configuration of the PV modules within a PV array instead of directly controlling a power converter.

5. CONCLUSIONS

The power-voltage curves of PV modules/arrays exhibit a point where the PV-generated power is maximized. Under uniform solar irradiation conditions, this point is unique, while in the case that different amounts of solar irradiation are incident on the individual PV modules of the PV array, multiple local MPPs also exist. Thus the control unit of the PV energy conversion system must execute an MPPT process to operate the PV source at the point where the generated power is maximized. This process enables optimal exploitation of the installed PV capacity, thus increasing the energy conversion efficiency of the overall PV system and, simultaneously, enhancing the economic benefit obtained during the PV system lifetime period.

The P&O and DMPPT methods have already been incorporated into commercial PV power converters [89, 90]. However, a wide variety of methods have additionally been proposed in the scientific literature during the last years for performing the MPPT process in a PV system. Targeting to assist the designers of PV power processing systems to select the most suitable MPPT method, the operational characteristics and implementation requirements of these techniques have been analyzed in this article.

In the case when the PV system may operate under non-uniform solar irradiation conditions, then the MPPT methods, which have been developed for PV arrays operating under uniform solar irradiation conditions, should not be applied, since they do not guarantee that the global MPP will be derived.

The operational complexity of each MPPT method affects the implementation cost of the corresponding control unit. Digital control units are most frequently employed in the modern PV power processing systems. The MPPT techniques relying on the execution of an optimization algorithm (*e.g.*, P&O, InC, evolutionary algorithms, etc.) are more easily integrated into such devices compared to the techniques that require the addition of specialized analog and/or digital control circuits for their operation. Thus, the economic burden imposed on the cost of the total PV power processing interface is minimized, and its flexibility to adapt to different operating conditions (*e.g.*, installation in alternative sites) is increased. Also, MPPT methods that require knowledge of one or more operational characteristics of the PV source, either regarding its configuration (*e.g.*, number of PV modules connected in series) or its operational parameters (*e.g.*, temperature coefficients, open-circuit voltage, etc.), are not suitable for incorporation in commercial PV power management products. In such a case, the specifications of the target PV source are not known during the design and manufacturing stages of the power converter and associated control unit, but they will be defined by the PV system designer considering the specific target application requirements. Furthermore, the accuracy of MPPT methods that operate by using the values of electrical parameters of the PV source is affected by (i) the uncertainty of the estimated electrical parameter values for the specific PV modules employed in each PV installation (*e.g.*, due to measurement errors during an experimental characterization process, deviation of the actual operating characteristics from the corresponding datasheet information, etc.), (ii) electrical parameters deviation among the individual PV modules supplied by a manufacturer due to non-idealities of the manufacturing process, and (iii) drift of the PV module electrical characteristics during the operational lifetime period of a PV system (*e.g.*, 25 years).

Each MPPT method also exhibits a different speed of deriving the MPP of the PV source. However, the intensity of the quantitative impact of this feature on the energy production performance of a PV system depends on the magnitude

and duration of the short-term variability of solar irradiation and ambient temperature at each particular installation site under consideration. Thus, to select an MPPT method for incorporation into a PV energy management system, its performance should be evaluated in terms of the total energy produced by the PV source under both static and dynamic operating conditions, considering the time-varying profile of the meteorological conditions that prevail during the year at the installation site of interest. Testing procedures that are suitable for evaluating and comparing the performance of MPPT algorithms were presented in [91, 92]. As analyzed in [93], the reliability of the software and hardware components of the MPPT control unit also affects the energy production of the PV system; thus, it must also be considered during the performance evaluation process of an MPPT method.

REFERENCES

[1] European Photovoltaic Industry Association, "Global market outlook for photovoltaics 2014-2018," 2014, available online at: www.epia.org

[2] Koutroulis, E., Kalaitzakis, K., and Voulgaris, N. C., "Development of a microcontroller-based, photovoltaic maximum power point tracking control system," *IEEE Trans. Power Electron.*, Vol. 16, No. 1, pp. 46–54, 2001.

[3] Kjaer, S. B., Pedersen, J. K., and Blaabjerg, F., "A review of single-phase grid-connected inverters for photovoltaic modules," *IEEE Trans. Ind. Appl.*, Vol. 41, No. 5, pp. 1292–1306, 2005.

[4] Koutroulis, E., and Blaabjerg, F., "A new technique for tracking the global maximum power point of PV arrays operating under partial-shading conditions," *IEEE J. Photovolt.*, Vol. 2, No. 2, pp. 184–190, 2012.

[5] Yang, Y., Wang, H., Blaabjerg, F., and Kerekes, T., "A hybrid power control concept for PV inverters with reduced thermal loading," *IEEE Trans. Power Electron.*, Vol. 29, No. 12, pp. 6271–6275, 2014.

[6] Bastidas-Rodriguez, J. D., Franco, E., Petrone, G., Andrés Ramos-Paja, C., and Spagnuolo, G., "Maximum power point tracking architectures for photovoltaic systems in mismatching conditions: A review," *IET Power Electron.*, Vol. 7, No. 6, pp. 1396–1413, 2014.

[7] Esram, T., and Chapman, P. L., "Comparison of photovoltaic array maximum power point tracking techniques," *IEEE Trans. Energy Convers.*, Vol. 22, No. 2, pp. 439–449, 2007.

[8] Ali, A. N. A., Saied, M. H., Mostafa, M. Z., and Abdel-Moneim, T. M., "A survey of maximum PPT techniques of PV systems," *2012 IEEE EnergyTech*, pp. 1–17, Cleveland, OH, 29–31 May 2012.

[9] Subudhi, B., and Pradhan, R., "A comparative study on maximum power point tracking techniques for photovoltaic power systems," *IEEE Trans. Sustain. Energy*, Vol. 4, No. 1, pp. 89–98, 2013.

[10] Liu, Y.-H., Chen, J.-H., and Huang, J.-W., "A review of maximum power point tracking techniques for use in partially shaded conditions," *Renew. Sustain. Energy Rev.*, Vol. 41, pp. 436–453, 2015.

[11] Ishaque, K., and Salam, Z., "A review of maximum power point tracking techniques of PV system for uniform insolation and partial shading condition," *Renew. Sustain. Energy Rev.*, Vol. 19, pp. 475–488, 2013.

[12] Eltawil, M. A., and Zhao, Z., "MPPT techniques for photovoltaic applications," *Renew. Sustain. Energy Rev.*, Vol. 25, pp. 793–813, 2013.

[13] Lorenzo, E., *Solar Electricity: Engineering of Photovoltaic Systems*," 1st ed., Seville, Spain: Progensa, Chap. 2, pp. 59–86, 1994.

[14] Kaa, G., Rezaei, J., Kamp, L., and Winter, A., "Photovoltaic technology selection: A fuzzy MCDM approach," *Renew. Sustain. Energy Rev.*, Vol. 32, pp. 662–670, 2014.

[15] International Energy Agency, "Technology roadmap—solar photovoltaic energy," 2014 edition, available online at: www.iea.org

[16] Jordan, D. C., and Kurtz, S. R., "Photovoltaic degradation rates—an analytical review," *Progr. Photovol. Res. Appl.*, Vol. 21, No. 1, pp. 12–29, 2013.

[17] de Wild-Scholten, M. J., "Energy payback time and carbon footprint of commercial photovoltaic systems," *Solar Energy Mater. Solar Cells*, Vol. 119, pp. 296–305, 2013.

[18] Laudani, A., Fulginei, F. R., and Salvini, A., "Identification of the one-diode model for photovoltaic modules from datasheet values," *Solar Energy*, Vol. 108, pp. 432–446, 2014.

[19] Cristaldi, L., Faifer, M., Rossi, M., and Toscani, S., "An improved model-based maximum power point tracker for photovoltaic panels," *IEEE Trans. Instrumentat. Measur.*, Vol. 63, No. 1, pp. 63–71, 2014.

[20] Tauseef, M., and Nowicki, E., "A simple and cost effective maximum power point tracker for PV arrays employing a novel constant voltage technique," *25th IEEE Canadian Conference on Electrical & Computer Engineering (CCECE)*, pp. 1–4, Montreal, QC, Canada, 29 April–2 May 2012.

[21] Ramasamy, A., and Vanitha, N. S., "Maximum power tracking for PV generating system using novel optimized fractional order open circuit voltage—FOINC method," *International Conference on Computer Communication and Informatics (ICCCI)*, pp. 1–6, Coimbatore, 3–5 January 2014.

[22] Di, X., Yundong, M., and Qianhong, C., "A global maximum power point tracking method based on interval short-circuit current," *16th European Conference on Power Electronics and Applications (EPE'14-ECCE Europe)*, pp. 1–8, Lappeenranta, 26–28 August 2014.

[23] El Khateb, A., Abd Rahim, N., Selvaraj, J., and Uddin, M. N., "Fuzzy-logic-controller-based SEPIC converter for maximum power point tracking," *IEEE Trans. Ind. Appl.*, Vol. 50, No. 4, pp. 2349–2358, 2014.

[24] Hua, C., Lin, J., and Shen, C., "Implementation of a DSP-controlled photovoltaic system with peak power tracking," *IEEE Trans. Ind. Electron.*, Vol. 45, No. 1, pp. 99–107, 1998.

[25] Femia, N., Petrone, G., Spagnuolo, G., and Vitelli, M., "A technique for improving P&O MPPT performances of double-stage grid-connected photovoltaic systems," *IEEE Trans. Ind. Electron.*, Vol. 56, No. 11, pp. 4473–4482, 2009.

[26] Ricco, M., Manganiello, P., Petrone, G., Monmasson, E., and Spagnuolo, G., "FPGA-based implementation of an adaptive

P&O MPPT controller for PV applications," *IEEE 23rd International Symposium on Industrial Electronics (ISIE)*, pp. 1876–1881, Istanbul, 1–4 June 2014.

[27] Kollimalla, S. K., and Mishra, M. K., "Variable perturbation size adaptive P&O MPPT algorithm for sudden changes in irradiance," *IEEE Trans. Sustain. Energy*, Vol. 5, No. 3, pp. 718–728, 2014.

[28] Huynh, D. C., Nguyen, T. A. T., Dunnigan, M. W., and Mueller, M. A., "Maximum power point tracking of solar photovoltaic panels using advanced perturbation and observation algorithm," *8th IEEE Conference on Industrial Electronics and Applications (ICIEA)*, pp. 864–869, Melbourne, VIC, 19–21 June 2013.

[29] Elgendy, M. A., Zahawi, B., and Atkinson, D. J., "Assessment of the incremental conductance maximum power point tracking algorithm," *IEEE Trans. Sustain. Energy*, Vol. 4, No. 1, pp. 108–117, 2013.

[30] Rahman, N. H. A., Omar, A. M., and Saat, E. H. M., "A modification of variable step size INC MPPT in PV system," *IEEE 7th International Power Engineering and Optimization Conference (PEOCO)*, pp. 340–345, Langkawi, 3–4 June 2013.

[31] Sera, D., Mathe, L., Kerekes, T., Spataru, S. V., and Teodorescu, R., "On the perturb-and-observe and incremental conductance MPPT methods for PV systems," *IEEE J. Photovol.*, Vol. 3, No. 3, pp. 1070–1078, 2013.

[32] Blanes, J. M., Toledo, F. J., Montero, S., and Garrigós, A., "In-site real-time photovoltaic I–V curves and maximum power point estimator," *IEEE Trans. Power Electron.*, Vol. 28, No. 3, pp. 1234–1240, 2013.

[33] Raj, J. S. C. M., and Jeyakumar, A. E., "A novel maximum power point tracking technique for photovoltaic module based on power plane analysis of characteristics," *IEEE Trans. Ind. Electron.*, Vol. 61, No. 9, pp. 4734–4745, 2014.

[34] Farivar, G., Asaei, B., and Mehrnami, S., "An analytical solution for tracking photovoltaic module MPP," *IEEE J. Photovolt.*, Vol. 3, No. 3, pp. 1053–1061, 2013.

[35] Bhatnagar, P., and Nema, R. K., "Maximum power point tracking control techniques: State-of-the-art in photovoltaic applications," *Renew. Sustain. Energy Rev.*, Vol. 23, pp. 224–241, 2013.

[36] Hartmann, L. V., Vitorino, M. A., Correa, M. B. R., and Lima, A. M. N., "Combining model-based and heuristic techniques for fast tracking the maximum-power point of photovoltaic systems," *IEEE Trans. Power Electron.*, Vol. 28, No. 6, pp. 2875–2885, 2013.

[37] Charfi, S., and Chaabene, M., "A comparative study of MPPT techniques for PV systems," *5th International Renewable Energy Congress (IREC)*, pp. 1–6, Hammamet, 25–27 March 2014.

[38] Afghoul, H., Krim, F., Chikouche, D., and Beddar, A., "Tracking the maximum power from a PV panels using of neuro-fuzzy controller," *IEEE International Symposium on Industrial Electronics (ISIE)*, pp. 1–6, Taipei, Taiwan, 28–31 May 2013.

[39] Sheraz, M., and Abido, M. A., "An efficient approach for parameter estimation of PV model using DE and fuzzy based MPPT controller," *IEEE Conference on Evolving and Adaptive Intelligent Systems (EAIS)*, pp. 1–5, Linz, Austria, 2–4 June 2014.

[40] Adly, M., and Besheer, A. H., "An optimized fuzzy maximum power point tracker for stand alone photovoltaic systems: Ant colony approach," *7th IEEE Conference on Industrial Electronics and Applications (ICIEA)*, pp. 113–119, Singapore, 18–20 July 2012.

[41] Veerachary, M., and Shinoy, K. S., "V2-based power tracking for nonlinear PV sources," *IEE Proc. Electr. Power Appl.*, Vol. 152, No. 5, pp. 1263–1270, 2005.

[42] Choi, B.-Y., Jang, J.-W., Kim, Y.-H., Ji, Y.-H., Jung, Y.-C., and Won, C.-Y., "Current sensorless MPPT using photovoltaic AC module-type flyback inverter," *IEEE International Symposium on Industrial Electronics (ISIE)*, pp. 1–6, Taipei, Taiwan, 28–31 May 2013.

[43] Agrawal, J., and Aware, M., "Golden section search (GSS) algorithm for maximum power point tracking in photovoltaic system," *IEEE 5th India International Conference on Power Electronics (IICPE)*, pp. 1–6, Delhi, 6–8 December 2012.

[44] Shao, R., Wei, R., and Chang, L., "A multi-stage MPPT algorithm for PV systems based on golden section search method," *29th Annual IEEE Applied Power Electronics Conference and Exposition (APEC)*, pp. 676–683, Fort Worth, TX, 16–20 March 2014.

[45] Xu, W., Mu, C., and Jin, J., "Novel linear iteration maximum power point tracking algorithm for photovoltaic power generation," *IEEE Trans. Appl. Superconduct.*, Vol. 24, No. 5, 2014.

[46] Pai, F.-S., Chao, R.-M., Ko, S. H., and Lee, T.-S., "Performance evaluation of parabolic prediction to maximum power point tracking for PV array," *IEEE Trans. Sustain. Energy*, Vol. 2, No. 1, pp. 60–68, 2011.

[47] Carraro, M., Costabeber, A., and Zigliotto, M., "Convergence analysis and tuning of ripple correlation based MPPT: A sliding mode approach," *15th European Conference on Power Electronics and Applications (EPE)*, pp. 1–10, Lille, 2–6 September 2013.

[48] Esram, T., Kimball, J. W., Krein, P. T., Chapman, P. L., and Midya, P., "Dynamic maximum power point tracking of photovoltaic arrays using ripple correlation control," *IEEE Trans. Power Electron.*, Vol. 21, No. 5, pp. 1282–1291, 2006.

[49] Barth, C. B., and Pilawa-Podgurski, R. C. N., "Dithering digital ripple correlation control with digitally-assisted windowed sensing for solar photovoltaic MPPT," *29th Annual IEEE Applied Power Electronics Conference and Exposition (APEC)*, pp. 1738–1746, Fort Worth, TX, 16–20 March 2014.

[50] Moo, C., and Wu, G., "Maximum power point tracking with ripple current orientation for photovoltaic applications," *IEEE J. Emerging Selected Topics Power Electroni.*, Vol. 2, No. 4, pp. 842–848, 2014.

[51] Li, X., Li, Y., and Seem, J. E., "Maximum power point tracking for photovoltaic system using adaptive extremum seeking control," *IEEE Trans. Control Syst. Technol.*, Vol. 21, No. 6, pp. 2315–2322, 2013.

[52] Xiao, W., Elnosh, A., Khadkikar, V., and Zeineldin, H., "Overview of maximum power point tracking technologies for photovoltaic power systems," *37th Annual Conference of the IEEE Industrial Electronics Society (IECON 2011)*, pp. 3900–3905, Melbourne, VIC, 7–10 November 2011.

[53] Zazo, H., Leyva, R., and del Castillo, E., "MPPT based on Newton-like extremum seeking control," *IEEE International*

Symposium on Industrial Electronics (ISIE), pp. 1040–1045, Hangzhou, 28–31 May 2012.

[54] Bazzi, A. M., and Krein, P. T., "Ripple correlation control: An extremum seeking control perspective for real-time optimization," *IEEE Trans. Power Electron.*, Vol. 29, No. 2, pp. 988–995, 2014.

[55] Malek, H., and Chen, Y., "A single-stage three-phase grid-connected photovoltaic system with fractional order MPPT," *29th Annual IEEE Applied Power Electronics Conference and Exposition (APEC)*, pp. 1793–1798, Fort Worth, TX, 16–20 March 2014.

[56] Levron, Y., and Shmilovitz, D., "Maximum power point tracking employing sliding mode control," *IEEE Trans. Circuits Syst. I: Reg. Papers*, Vol. 60, No. 3, pp. 724–732, 2013.

[57] Cheng, Z., Pang, Z., Liu, Y., and Xue, P., "An adaptive solar photovoltaic array reconfiguration method based on fuzzy control," *8th World Congress on Intelligent Control and Automation (WCICA)*, pp. 176–181, Jinan, 7–9 July 2010.

[58] Daraban, S., Petreus, D., and Morel, C., "A novel global MPPT based on genetic algorithms for photovoltaic systems under the influence of partial shading," *39th Annual Conference of the IEEE Industrial Electronics Society (IECON)*, pp. 1490–1495, Vienna, 10–13 November 2013.

[59] Taheri, H., Salam, Z., Ishaque, K., and Syafaruddin, "A novel maximum power point tracking control of photovoltaic system under partial and rapidly fluctuating shadow conditions using differential evolution," *2010 IEEE Symposium on Industrial Electronics & Applications (ISIEA)*, pp. 82–87, Penang, 3–5 October 2010.

[60] Ishaque, K., and Salam, Z., "A deterministic particle swarm optimization maximum power point tracker for photovoltaic system under partial shading condition," *IEEE Trans. Ind. Electron.*, Vol. 60, No. 8, pp. 3195–3206, 2013.

[61] Liu, Y.-H., Huang, S.-C., Huang, J.-W., and Liang, W.-C., "A particle swarm optimization-based maximum power point tracking algorithm for PV systems operating under partially shaded conditions," *IEEE Trans. Energy Convers.*, Vol. 27, No. 4, pp. 1027–1035, 2012.

[62] Ting, T. O., Man, K. L., Guan, S.-U., Jeong, T. T., Seon, J. K., and Wong, P. W. H., "Maximum power point tracking (MPPT) via weightless swarm algorithm (WSA) on cloudy days," *IEEE Asia Pacific Conference on Circuits and Systems (APCCAS)*, pp. 336–339, Kaohsiung, 2–5 December 2012.

[63] Sundareswaran, K., Peddapati, S., and Palani, S., "MPPT of PV systems under partial shaded conditions through a colony of flashing fireflies," *IEEE Trans. Energy Convers.*, Vol. 29, No. 2, pp. 463–472, 2014.

[64] Lian, K. L., Jhang, J. H., and Tian, I. S., "A maximum power point tracking method based on perturb-and-observe combined with particle swarm optimization," *IEEE J. Photovolt.*, Vol. 4, No. 2, pp. 626–633, 2014.

[65] Bidram, A., Davoudi, A., and Balog, R. S., "Control and circuit techniques to mitigate partial shading effects in photovoltaic arrays," *IEEE J. Photovolt.*, Vol. 2, No. 4, pp. 532–546, 2012.

[66] Nguyen, T. L., and Low, K.-S., "A global maximum power point tracking scheme employing DIRECT search algorithm for photovoltaic systems," *IEEE Trans. Ind. Electron.*, Vol. 57, No. 10, pp. 3456–3467, 2010.

[67] Ahmed, N. A., and Miyatake, M., "A novel maximum power point tracking for photovoltaic applications under partially shaded insolation conditions," *Electr. Power Syst. Res.*, Vol. 78, No. 5, pp. 777–784, 2008.

[68] Sundareswaran, K., Peddapati, S., and Palani, S., "Application of random search method for maximum power point tracking in partially shaded photovoltaic systems," *IET Renew. Power Generat.*, Vol. 8, No. 6, pp. 670–678, 2014.

[69] Zhou, L., Chen, Y., Guo, K., and Jia, F., "New approach for MPPT control of photovoltaic system with mutative-scale dual-carrier chaotic search," *IEEE Trans. Power Electron.*, Vol. 26, No. 4, pp. 1038–1048, 2011.

[70] Konstantopoulos, C., and Koutroulis, E., "Global maximum power point tracking of flexible photovoltaic modules," *IEEE Trans. Power Electron.*, Vol. 29, No. 6, pp. 2817–2828, 2014.

[71] Sharma, P., Peter, P. K., and Agarwal, V., "Exact maximum power point tracking of partially shaded PV strings based on current equalization concept," *38th IEEE Photovoltaic Specialists Conference (PVSC)*, pp. 1411–1416, Austin, TX, 3–8 June 2012.

[72] Sharma, P., and Agarwal, V., "Comparison of model based MPPT and exact MPPT for current equalization in partially shaded PV strings," *IEEE 39th Photovoltaic Specialists Conference (PVSC)*, pp. 2948–2952, Tampa, FL, 16–21 June 2013.

[73] Sharma, P., and Agarwal, V., "Maximum power extraction from a partially shaded PV array using shunt-series compensation," *IEEE J. Photovolt.*, Vol. 4, No. 4, pp. 1128–1137, 2014.

[74] Sharma, P., and Agarwal, V., "Exact maximum power point tracking of grid-connected partially shaded PV source using current compensation concept," *IEEE Trans. Power Electron.*, Vol. 29, No. 9, pp. 4684–4692, 2014.

[75] Ramos-Paja, C. A., Spagnuolo, G., Petrone, G., Serna, S., and Trejos, A., "A vectorial MPPT algorithm for distributed photovoltaic applications," *International Conference on Clean Electrical Power (ICCEP)*, pp. 48–51, Alghero, 11–13 June 2013.

[76] Scarpetta, F., Liserre, M., and Mastromauro, R. A., "Adaptive distributed MPPT algorithm for photovoltaic systems," *38th Annual Conference of the IEEE Industrial Electronics Society (IECON)*, pp. 5708–5713, Montreal, QC, 25–28 October 2012.

[77] Ramli, M. Z., and Salam, Z., "A simple energy recovery scheme to harvest the energy from shaded photovoltaic modules during partial shading," *IEEE Trans. Power Electron.*, Vol. 29, No. 12, pp. 6458–6471, 2014.

[78] Alajmi, B. N., Ahmed, K. H., Finney, S. J., and Williams, B. W., "A maximum power point tracking technique for partially shaded photovoltaic systems in microgrids," *IEEE Trans. Ind. Electron.*, Vol. 60, No. 4, pp. 1596–1606, 2013.

[79] Yeung, R. S.-C., Chung, H. S.-H., and Chuang, S. T.-H., "A global MPPT algorithm for PV system under rapidly fluctuating irradiance," *29th Annual IEEE Applied Power Electronics Conference and Exposition (APEC)*, pp. 662–668, Fort Worth, TX, 16–20 March 2014.

[80] Boztepe, M., Guinjoan, F., Velasco-Quesada, G., Silvestre, S., Chouder, A., and Karatepe, E., "Global MPPT scheme for photovoltaic string inverters based on restricted voltage window search algorithm," *IEEE Trans. Ind. Electron.*, Vol. 61, No. 7, pp. 3302–3312, 2014.

[81] Hu, Y., Cao, W., Wu, J., Ji, B., and Holliday, D., "Thermography-based virtual MPPT scheme for improving PV energy efficiency under partial shading conditions," *IEEE Trans. Power Electron.*, Vol. 29, No. 11, pp. 5667–5672, 2014.

[82] Tey, K. S., and Mekhilef, S., "Modified incremental conductance algorithm for photovoltaic system under partial shading conditions and load variation," *IEEE Trans. Ind. Electron.*, Vol. 61, No. 10, pp. 5384–5392, 2014.

[83] Jiang, L. L., Nayanasiri, D. R., Maskell, D. L., and Vilathgamuwa, D. M., "A simple and efficient hybrid maximum power point tracking method for PV systems under partially shaded condition," *39th Annual Conference of the IEEE Industrial Electronics Society (IECON)*, pp. 1513–1518, Vienna, 10–13 November 2013.

[84] Bifaretti, S., Iacovone, V., Cina, L., and Buffone, E., "Global MPPT method for partially shaded photovoltaic modules," *IEEE Energy Conversion Congress and Exposition (ECCE)*, pp. 4768–4775, Raleigh, NC, 15–20 September 2012.

[85] Chen, J.-H., Cheng, Y.-S., Wang, S.-C., Huang, J.-W., and Liu, Y.-H., "A novel global maximum power point tracking method for photovoltaic generation system operating under partially shaded condition," *International Power Electronics Conference (IPEC)*, pp. 3233–3238, Hiroshima, 18–21 May 2014.

[86] Chen, K., Tian, S., Cheng, Y., and Bai, L., "An improved MPPT controller for photovoltaic system under partial shading condition," *IEEE Trans. Sustain. Energy*, Vol. 5, No. 3, pp. 978–985, 2014.

[87] Lei, P., Li, Y., and Seem, J. E., "Sequential ESC-based global MPPT control for photovoltaic array with variable shading," *IEEE Trans. Sustain. Energy*, Vol. 2, No. 3, pp. 348–358, 2011.

[88] Elnosh, A., Khadkikar, V., Xiao, W., and Kirtely, J. L., "An improved extremum-seeking based MPPT for grid-connected PV systems with partial shading," *IEEE 23rd International Symposium on Industrial Electronics (ISIE)*, pp. 2548–2553, Istanbul, 1–4 June 2014.

[89] Hohm, D. P., and Ropp, M. E., "Comparative study of maximum power point tracking algorithms," *Progr. Photovolt. Res. Appl.*, Vol. 11, No. 1, pp. 47–62, 2003.

[90] Petrone, G., Spagnuolo, G., and Vitelli, M., "Distributed maximum power point tracking: challenges and commercial solutions," *Automatika*, Vol. 53, No. 2, pp. 128–141, 2012.

[91] Valentini, M., Raducu, A., Sera, D., and Teodorescu, R., "PV inverter test setup for European efficiency, static and dynamic MPPT efficiency evaluation," *11th International Conference on Optimization of Electrical and Electronic Equipment (OPTIM)*, pp. 433–438, Brasov, 22–24 May 2008.

[92] Xiao, W., Zeineldin, H. H., and Zhang, P., "Statistic and parallel testing procedure for evaluating maximum power point tracking algorithms of photovoltaic power systems," *IEEE J. Photovolt.*, Vol. 3, No. 3, pp. 1062–1069, 2013.

[93] Zhang, P., Li, W., Li, S., Wang, Y., and Xiao, W., "Reliability assessment of photovoltaic power systems: Review of current status and future perspectives," *Appl. Energy*, Vol. 104, pp. 822–833, 2013.

BIOGRAPHIES

Eftichios Koutroulis received his B.Sc. and M.Sc. from the School of Electronic and Computer Engineering of the Technical University of Crete (Chania, Greece) in 1996 and 1999, respectively. He received his Ph.D. from the School of Electronic and Computer Engineering of the Technical University of Crete in 2002, in the area of power electronics and renewable energy sources (RES). He is currently an assistant professor at the School of Electronic and Computer Engineering of the Technical University of Crete. His current research interests include power electronics (DC/AC inverters, DC/DC converters), the development of microelectronic energy management systems for RES, and the design of photovoltaic and wind energy conversion systems.

Frede Blaabjerg was with ABB-Scandia, Randers, Denmark, from 1987 to 1988. From 1988 to 1992, he was a Ph.D. student with Aalborg University, Aalborg, Denmark. He became an assistant professor in 1992, an associate professor in 1996, and a full professor of power electronics and drives in 1998. He has received 15 IEEE Prize Paper Awards, the IEEE PELS Distinguished Service Award in 2009, the EPE-PEMC Council Award in 2010, the IEEE William E. Newell Power Electronics Award in 2014, and the Villum Kann Rasmussen Research Award in 2014. An IEEE Fellow, he was the editor-in-chief of *IEEE Transactions on Power Electronics* from 2006 to 2012. He has been a distinguished lecturer for the IEEE Power Electronics Society from 2005 to 2007 and for the IEEE Industry Applications Society from 2010 to 2011. He was nominated in 2014 by Thomson Reuters to be among the 250 most-cited researchers in engineering in the world. His current research interests include power electronics and its applications, such as in wind turbines, PV systems, reliability, harmonics, and adjustable speed drives.